

Dynamic Radio Resource Allocation in Wireless Sensor and Cognitive Radio Networks

A Thesis

Presented in Partial Fulfillment of the Requirements for
the Degree Master of Science in the
Graduate School of The Ohio State University

By

Suk-Un Yoon, M.S.
Graduate Program in Electrical and Computer Engineering

* * * * *

The Ohio State University

2009

Master's Examination Committee:

Eylem Ekici, Adviser

Bradley D. Clymer

© Copyright by

Suk-Un Yoon

2009

ABSTRACT

In wireless networks, it is required to change an operating frequency as part of the radio resource management due to strong interference or system requirements of accessing radio resources. In this thesis, we propose two radio resource management schemes in wireless sensor networks and cognitive radio networks. In the proposed schemes, sensor networks switch to a new channel when they detect strong interference and a secondary user in cognitive radio networks moves to a new spectrum when it detects or predicts the presence of a primary user.

In the first part of the thesis, we propose a channel hopping scheme which can be used for interfered wireless networks. With the additive functionality of a channel hopping mechanism on the sensor network stack, we aim to avoid the interference from other sensor nodes and wireless technologies on ISM band as well as avoid narrow-band jamming. For simple and reliable channel hopping, we introduce an *Adaptive Channel Hopping* scheme, a spectrum environment aware channel hopping scheme, for interference robust wireless sensor networks. When the channel status becomes suboptimal to communicate, the adaptive channel hopping lets the sensors switch to a new clean channel. To generate channel selection/scanning orders which minimize channel hopping latency, we use two parameters which are link quality indicator (LQI) and channel weighting. The proposed adaptive channel hopping scheme is evaluated through simulations. Simulation results indicate that

the proposed scheme significantly reduces the channel hopping latency and selects the best quality channel.

In the second part of the thesis, we propose a novel approach to spectrum management in cognitive radio networks. To support flexible use of spectrum, cognitive radio networks employ spectrum mobility management schemes, including spectrum handoff, which refers to the switching of the operating spectrum due to changes in licensed (primary) user activity. Spectrum handoff inevitably results in temporary disruption of communication for the unlicensed (secondary) user operating in a licensed band opportunistically. Minimization of secondary user service disruption is an important objective of spectrum handoff schemes. In this thesis, we introduce a new type of spectrum handoff called *Voluntary Spectrum Handoff* assisted by a primary user spectrum usage estimation scheme. The two mechanisms proposed under voluntary spectrum handoff method estimate opportune times to initiate unforced spectrum handoff events to facilitate setup and signaling of alternative channels without having communication disruption, which occurs when a secondary user is forced out of an operating spectrum due to primary user activity. To estimate primary user spectrum usage, channel usage information is continuously updated with a fixed spectrum sensing window and a variable history window. Proposed voluntary spectrum handoff and primary usage estimation schemes are evaluated through extensive simulations. Simulation results indicate that the proposed schemes significantly reduce the communication disruption duration due to handoffs.

This is dedicated to my wife, Se Eun Kim

ACKNOWLEDGMENTS

I would like to thank many people as I am studying in the Ohio State University. I would like to give my special gratitude to my wife, Se Eun Kim for her support, understanding, patience, and sacrifices.

I thank my advisor, Dr. Eylem Ekici for his advice and support throughout this study. I wish also thank my committee, Dr. Bradley D. Clymer for serving my committee.

I would also like to express my gratitude to ECE students and Korean students with whom I have enjoyed numerous fruitful discussions and spent memorable times.

VITA

Aug. 15, 1975 Born - Donghae, Korea

1994 - 1998 B.S. Electronics Engineering,
Soongsil University, Seoul, Korea

1998 - 2001 M.S. Electronics Engineering,
Korea University, Seoul, Korea

Jan. 2001 - Jul. 2007 Senior Software Engineer,
Samsung Electronics, Sowon, Korea

2007-present Graduate Student,
The Ohio State University.

PUBLICATIONS

Research Publications

Suk-Un Yoon, Robert Murawski, Eylem Ekici, Sangjoon Park, and Zeeshan Hameed Mir, “Adaptive Channel Hopping for Interference Robust Wireless Sensor Networks”. *Submitted to IEEE ICC 2010*

Suk-Un Yoon and Eylem Ekici, “Voluntary Spectrum Handoff: A Novel Approach to Spectrum Management in Cognitive Radio Networks”. *Submitted to IEEE ICC 2010*

FIELDS OF STUDY

Major Field: Electrical and Computer Engineering

TABLE OF CONTENTS

	Page
Abstract	ii
Dedication	iv
Acknowledgments	v
Vita	vi
List of Tables	ix
List of Figures	x
Chapters:	
1. Introduction	1
1.1 Radio Resource Management	1
1.2 Adaptive Channel Hopping in Wireless Sensor Networks	3
1.2.1 Wireless Sensor Networks	3
1.2.2 ISM Interference to Sensor Networks	4
1.2.3 Objective	5
1.3 Voluntary Spectrum Handoff in Cognitive Radio Networks	5
1.3.1 Cognitive Radio Networks	5
1.3.2 Objective	7
2. Adaptive Channel Hopping	9
2.1 Architecture	9
2.1.1 Preliminaries	9
2.1.2 Network Model	10
2.1.3 Channel Classification	11

2.2	Adaptive Channel Hopping	14
2.2.1	Hopping Sequence Generation	14
2.2.2	Channel Hopping Algorithms	17
2.2.3	Packet Model and Channel Hopping Latency	21
2.3	Sensor Network Simulation and Results	24
2.3.1	Sensor Network Simulator	24
2.3.2	Channel Hopping Latency Measurement	25
2.3.3	Channel Hopping Latency Comparisons	29
2.3.4	Channel Hopping Latency Comparisons in Different Interference Levels	32
2.3.5	Throughput and Hopping Latency Comparisons	35
3.	Voluntary Spectrum Handoff	36
3.1	Cognitive Radio Networks	36
3.2	Architecture	38
3.2.1	Assumptions	39
3.2.2	Network Model	40
3.3	Spectrum Usage Estimation	41
3.3.1	Sensing Window Size Selection	42
3.3.2	Spectrum Usage Estimator	46
3.4	Spectrum Handoff Management	48
3.4.1	Voluntary Spectrum Handoff	48
3.4.2	Spectrum Lifetime Estimation	48
3.4.3	Voluntary Spectrum Handoff Process	51
3.5	Performance Evaluation	52
3.5.1	Spectrum Handoff Count Comparison	54
3.5.2	Communication Disruption Ratio Comparison	58
3.5.3	Effect of Primary User Spectrum Usage	58
4.	Conclusions and Future Work	64
	Bibliography	66

LIST OF TABLES

Table		Page
2.1	Parameters of the Packet Model	23
2.2	Throughput and Hopping Latency Comparisons	35
3.1	Traffic Source Parameters	54
3.2	Spectrum Handoff Counts	54

LIST OF FIGURES

Figure	Page
1.1 Radio Resource Management	2
2.1 Network Model	10
2.2 Superframe Structure	11
2.3 Typical RSSI value vs. input power [14]	12
2.4 Correlation between Average LQI and PRR [12]	13
2.5 Channel Classification	15
2.6 Hopping Sequence Generation	16
2.7 Channel Hopping Algorithm for Parent	18
2.8 Channel Hopping Algorithm for Children	19
2.9 An Example of Channel Locking Timing Diagram	22
2.10 Packet Model of IEEE 802.15.4 Sensor Networks	23
2.11 An Example of Transmission Delay	24
2.12 Wireless Network Simulator	26
2.13 Channel Hopping Latency	27
2.14 Channel Hopping Latency with Successful CHC Reception Ratio	28

2.15	Channel Hopping Latency Comparison	30
2.16	Latency Comparison with Command Message Interval Change	31
2.17	Common Clear Channel and Average Latency of ALQI	32
2.18	Latency Comparison with Different Levels of Interference	33
2.19	Latency Comparison with CM Interval and Different Interference Levels . .	34
3.1	FCC Spectrum Allocation [16]	37
3.2	Cognitive Radio Concept [19]	38
3.3	Network Model	40
3.4	Spectrum Usages	41
3.5	Spectrum Cycle Average Variance	44
3.6	Estimation Error with Sensing Window	45
3.7	Primary User Spectrum Usage Estimation	47
3.8	CDR Comparison for IM	56
3.9	CDR Comparison for DM	57
3.10	CDR Comparison for SM	58
3.11	CDR Comparison for HM	59
3.12	CDR Comparison with $E\{T_{OFF}\} = 3$	60
3.13	CDR Comparison with Various PU Traffic Parameters	61
3.14	CDR Comparison with RBS	63

CHAPTER 1

INTRODUCTION

1.1 Radio Resource Management

The rapid increase in the size of the wireless mobile community and its demands for high-speed multimedia communications stands in clear contrast to the rather limited spectrum resources that have been allocated in international agreements. Efficient spectrum or radio resource management (RRM) is of paramount importance due to these increasing demands [1]. Radio resource management techniques, as shown in Figure 1.1, including admission control, scheduling, subcarrier allocation, channel (radio resource) assignment, power allocation, and rate control are essential for maximizing the resource utilization and providing quality of service (QoS) in wireless networks [2]. In many cases, the performance metrics (e.g., overall throughput) can be optimized if opportunistic algorithms are employed. In most existing works on radio resource management, resource allocation/assignment is dealt with to get better performance metrics. We also propose the resource management (or allocation) techniques with view points of solving mutual interference problems or meeting the system requirements of accessing radio channels. In this thesis, the aim of radio resource management for wireless sensor networks and cognitive radio networks is to share the available and often rather limited radio resources between

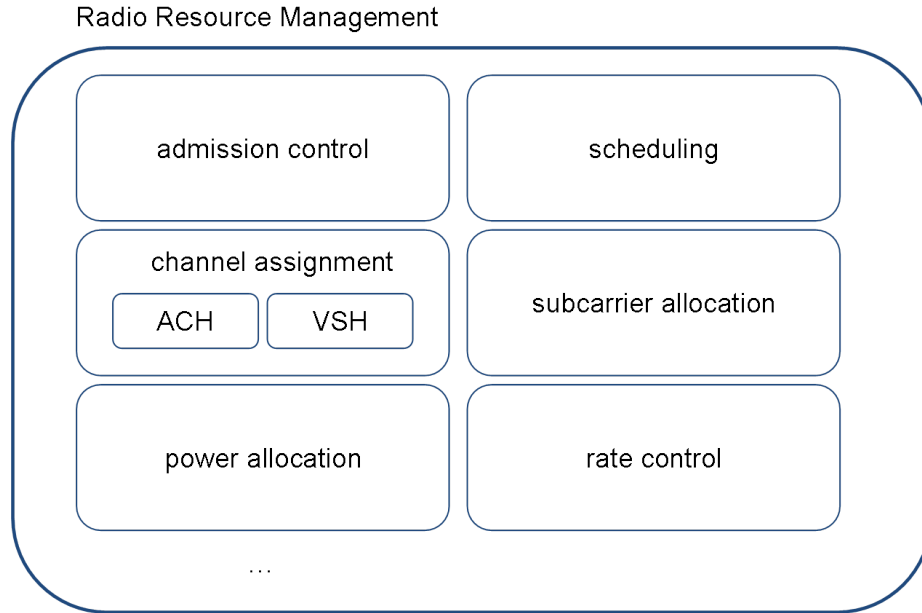


Figure 1.1: Radio Resource Management

users as efficiently as possible. Here, the efficiency refers to providing robust or undisturbed communication with respect to overcoming the fundamental difficulties of radio interference in wireless sensor networks and satisfying the system requirements in cognitive radio networks. For an interference robust resource management in wireless sensor networks, we introduce an *Adaptive Channel Hopping* scheme which is a spectrum environment aware channel hopping scheme. To minimize secondary user service disruption in cognitive radio networks, we introduce a new type of spectrum handoff called *Voluntary Spectrum Handoff* assisted by a primary user spectrum usage estimation scheme.

1.2 Adaptive Channel Hopping in Wireless Sensor Networks

1.2.1 Wireless Sensor Networks

A wireless sensor network is formed by a group of nodes that are capable of sensing one or more physical attributes of their environment such as temperature, light, sound, etc., processing and storing these sensed values locally and coordinating with other sensor nodes using their wireless radios. Additionally, some network nodes may also have actuation capabilities by which they can control or manipulate their physical environment. A typical characteristic of wireless sensor/actuator networks in their present day form, that distinguishes them from traditional networks such as the Internet, is that they are built out of low-cost, resource constrained components, following the general principle that although individual nodes may have limited capabilities and be subject to faults, their low cost makes deployments at large scales feasible. In real world, the standard organizations announced the standard sensor network protocols such as IEEE 802.15.4 [3] or ZigBee [4] and industrial companies such as Texas Instrument produced a single-chip 2.4 GHz IEEE 802.15.4 compliant RF transceiver such as CC2420 [14] for wireless applications.

ZigBee [4] has been designed as a standardized solution for sensor and control networks. Most ZigBee devices are extremely power-sensitive (thermostats, security sensors, etc.) with target battery life being measured in years. ZigBee uses a DSSS radio signal in the 868 MHz band (Europe), 915 MHz band (North America), and the 2.4 GHz ISM band (available worldwide) [6]. In the 2.4-GHz ISM band sixteen channels are defined; each channel occupies 3 MHz and channels are centered 5 MHz from each other, giving a 2-MHz gap between pairs of channels. ZigBee uses an 11-chip PN code, with 4 information bits encoded into each symbol giving it a maximum data rate of 128 Kbps. The physical

and MAC layers are defined by the IEEE 802.15.4 Working Group and share many of the same design characteristics as the IEEE 802.11b standard.

1.2.2 ISM Interference to Sensor Networks

Today, there are many devices produced that operate within the unlicensed industrial, scientific and medical (ISM) band. Commercially available sensor networks that operate within the ISM band must have the ability to compensate for local interference or they can potentially suffer performance degradation or even network loss. To achieve the best performance in homogeneous and heterogeneous environments, each ISM-based solution implements its own interference avoidance technology. In the 2.4 GHz ISM band, Wi-Fi, WirelessUSB, and 802.15.4 [3] (known as ZigBee [4] when combined with the upper networking layers) use direct-sequence spread spectrum (DSSS) while Bluetooth uses frequency-hopping spread spectrum (FHSS) [22]. Wi-Fi utilizes carrier sense multiple access (CSMA) that listens to the medium prior to transmission to reduce the probability of collisions. Bluetooth specification version 1.2 defines an adaptive frequency hopping algorithm which allows Bluetooth devices to mark channels as good, bad, or unknown and utilizes only the channels that are of good quality. WirelessUSB devices use a fixed channel, but dynamically change channels if the link quality of the original channel becomes suboptimal. ZigBee provides a collision-avoidance algorithm similar to Wi-Fi; each ZigBee device listens to the channel before transmitting in order to minimize collisions between devices [22, 6]. To minimize data loss caused by collisions, ZigBee relies upon its low duty cycle and collision-avoidance algorithms, but does not change channels, which is insufficient to avoid heavy interference or narrow-band jamming.

1.2.3 Objective

When considering the coexistence of wireless sensor networks (WSNs) and other ISM-based solutions such as Wi-Fi, one of the main concerns is performance degradation due to local interference. This issue has been researched for large scale 802.15.4 multi-hop sensor networks. In [7] the authors propose an adaptive radio channel allocation scheme which allows nodes experiencing significant interference to switch to new frequency channels with less congestion. To minimize the effect of Wi-Fi interference in 802.15.4 WSNs, an interference detection and avoidance mechanism is proposed which selects the radio channel that is least likely to have interference before each download operation [8]. To minimize interference of 802.11b/g, frequency hopping schemes that utilize the four guard channels of IEEE 802.11b/g have been proposed. The results show that frequency hopping can be used as a reliable interference avoidance mechanism to facilitate coexistence in 802.15.4 networks [9]. In this thesis, we propose *Adaptive Channel Hopping*, a simple and reliable channel hopping algorithm that can be applied to existing sensor network standards. The algorithm has been evaluated through extensive simulations.

1.3 Voluntary Spectrum Handoff in Cognitive Radio Networks

1.3.1 Cognitive Radio Networks

With the growing number of wireless devices and increased spectrum occupancy, the unlicensed spectrum is getting scarce. Additionally, large portions of the licensed spectrum, even in urban areas, are underutilized [17]. To address the potential spectrum exhaustion problem, new wireless communication paradigms have been proposed for future wireless communication devices. The Cognitive Radio (CR) concept is a new wireless communication paradigm that improves the spectrum usage efficiency by exploiting the existence of

spectrum holes [18]. Devices using CRs referred to as Secondary Users (SUs), are aware of their spectrum environments and change their transmission and reception parameters to avoid interference with licensed spectrum users referred to as Primary Users (PUs). Networks consisting of nodes equipped with CRs are referred to as Cognitive Radio Networks (CRNs) [19, 20]. CRNs are networks that have cognitive and reconfigurable properties and the capability to detect unoccupied spectrum holes and change frequency for end-to-end communication [19, 21, 22]. In most of the existing proposals, CRNs employ three steps of basic functionality. Observing and sensing is the first step of the cognitive process. The next step is to identify and analyze the spectrum. The last step is sharing the spectrum information and executing spectrum assignment. In addition to these awareness functionalities, to maintain seamless communication, several proposals envision *spectrum mobility* which is caused by three reasons such as PU detection, channel degradation, and SU mobility [19, 23].

In CRNs, spectrum mobility causes a new type of handoff referred to as *spectrum handoff* [19], which is different from traditional cellular handoff and mainly caused by the presence of PUs. In cellular networks, mobile devices transfer an ongoing connection from one channel to another channel between base stations due to user mobility or channel degradation. However, the concept of user movement has also new meanings in CRNs because the number and characteristic of available spectrum at a new location may vary with PU spectrum usage. Moreover, the spectrum handoffs in CRNs are likely to incur longer delays or temporary communication disruptions because SUs must search for spectrum holes and choose a proper channel at every spectrum handoff. In [23], research issues related to spectrum handoff are introduced. Sensing and assignment of available spectrum are important functions for spectrum handoff in dynamic spectrum access networks. To sense and

discover spectrum holes which have long lifetimes, probabilistic and adaptive spectrum sensing algorithms have been reported in several publications [24, 25, 26]. For opportunistic spectrum discovery, sensing-period adaptation and optimal sensing-sequencing schemes at channel switching are presented in [24]. A BTR (Busy Time Ratio)-based channel quality metric and a distributed measurement scheme are proposed in [25]. With the sensing results of the spectrum holes, the unused channels can be assigned to SUs. To accomplish channel assignment, opportunistic access schemes including frequency hopping are explored in [27]. In spectrum mobility management, spectrum sharing is also an important step to discover a commonly available channel on both transmitter and receiver SUs. To share sensing information and to setup communication links, common control channel concepts are advocated in [28, 29].

1.3.2 Objective

In this thesis, we propose a new type of spectrum handoff referred to as *Voluntary Spectrum Handoff (VSH)* to reduce temporary communication disruption time which is caused by spectrum handoffs. VSH is not necessarily triggered by PU detection as in conventional spectrum handoff referred to as Forced Spectrum Handoff (FSH) in this thesis. Estimating remaining time until PU spectrum access, SUs voluntarily change the spectrum without conflicting with PUs. By voluntarily changing the spectrum at estimated times, SUs can reduce time delays caused by spectrum hole search and spectrum information sharing by overlapping these functions in time with data communication. For the estimation of PU spectrum usage, we define two spectrum sensing periods, i.e., a fixed spectrum sensing window and a variable history window. To select an optimal channel which is currently unused and has the longest spectrum lifetime, we propose two spectrum selection

algorithms called Transition Probability Selection (TPS) and Reliability Based Selection (RBS). The proposed spectrum usage estimation method and spectrum selection algorithms can be used for arbitrary probability distributions. VSH reverts back to FSH in case a primary user accesses a spectrum currently used by an SU before a VSH occurs. Simulation results show that SUs have shorter communication disruption durations with VSH.

CHAPTER 2

ADAPTIVE CHANNEL HOPPING

With the additive functionality of a channel hopping mechanism on wireless sensor networks stack, we want to avoid the interference from other nodes and technologies on ISM band. For a channel hopping, we introduce *Adaptive Channel Hopping* (ACH) scheme, a spectrum environment aware channel hopping scheme, for interference robust wireless sensor networks. When the channel status becomes suboptimal to communicate, the adaptive channel hopping lets the sensors switch to a new clean channel. To generate channel selection/scanning orders which minimize channel hopping latency, we use two parameters which are link quality indicator (LQI) and channel weighting.

2.1 Architecture

2.1.1 Preliminaries

In this thesis, we utilize a pre-defined sequence of communication channels that represent a given portion of the unlicensed ISM band. All nodes have a single communication interface and run-time channel selection capability via software configuration. All nodes are of similar hardware and configuration as described below in the following section.

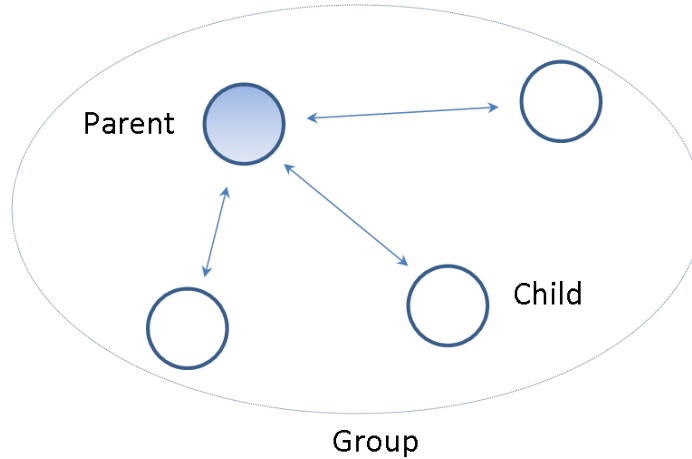


Figure 2.1: Network Model

2.1.2 Network Model

Our system model consists of multiple wireless devices which are organized into groups. Each group contains a single parent and one or more child nodes as shown in Figure 2.1. For the purposes of this research, the parent node is the coordinator for all frequency hopping events. Our algorithm is applicable to MAC layer protocols that have the following properties: time synchronization, neighbor discovery, and the ability to organize users into separate timeslots for channel hop synchronization. Such protocols include 802.15.4 (or Zigbee) and Sector Antenna MAC (SAMAC) [15] given a single-hop network topology. We assume that spatial reuse is utilized to reduce the number of timeslots required for a given network topology. Combining all $N_{timeslot}$ timeslots within a network forms a superframe as shown in Figure 2.2 that is repeated every $N_{timeslot} \times t_{timeslot}$ seconds,

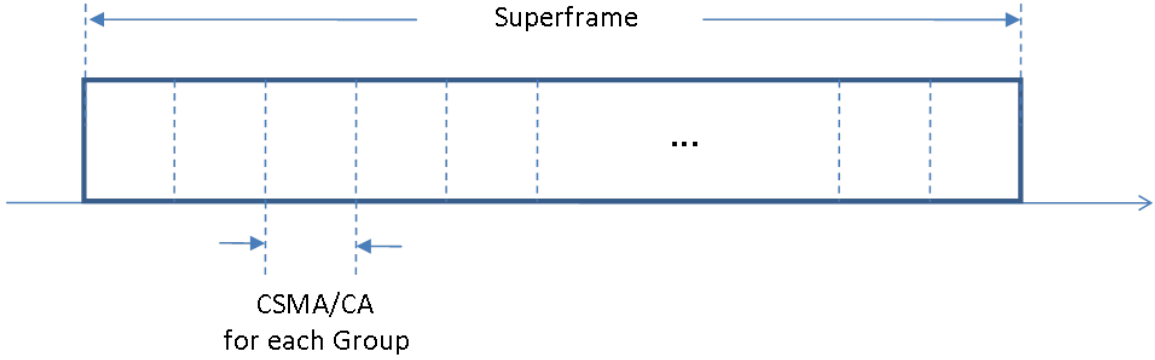


Figure 2.2: Superframe Structure

where $t_{timeslot}$ is the duration of each timeslot. For this research, we assume that the timeslot schedules in which a group of nodes become active are available at all nodes using the Adaptive Channel Hopping scheme.

2.1.3 Channel Classification

The channels are classified by the link quality indicator (LQI). The LQI measurement is a characterization of the strength or/and quality of a received packet. The measurement can be implemented using receiver energy detection (ED)/received signal strength indicator (RSSI), a signal-to-noise ratio estimation, or a combination of these methods. When energy level and SNR data are combined, they can indicate whether a corrupt packet resulted from low signal strength or from high signal strength plus interference. The RSSI value may be used by the MAC software to produce the LQI value. CC2420 [14] has a built-in RSSI giving a digital value that can be read from the 8 bit, signed 2^7 's complement RSSI.RSSI-VAL register. The RSSI value is always averaged over 8 symbol periods ($128 \mu s$). The RSSI-VALID status bit indicates when the RSSI value is valid, meaning that the receiver has

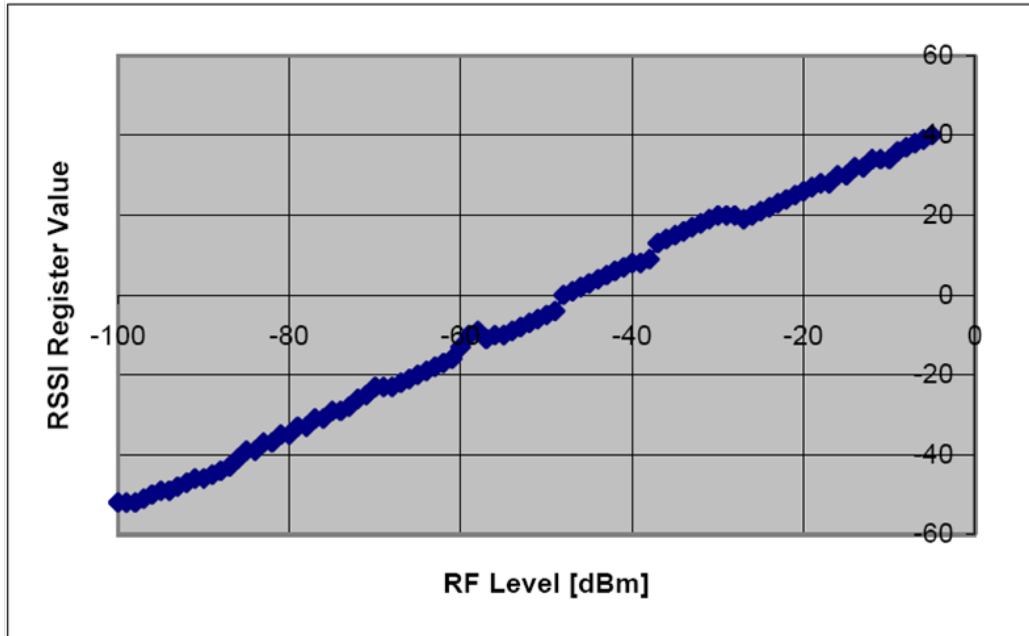


Figure 2.3: Typical RSSI value vs. input power [14]

been enabled for at least 8 symbol periods. The RSSI register value `RSSI.RSSI-VAL` can be referred to the power P at the RF pins by using the following equations: $P = \text{RSSI-VAL} + \text{RSSI-OFFSET}$ [dBm], where the `RSSI-OFFSET` is found empirically during system development from the front end gain. `RSSI-OFFSET` is approximately -45 . E.g. if reading a value of -20 from the RSSI register, the RF input power is approximately -65 dBm. A typical plot of the `RSSI-VAL` reading as function of input power is shown in Figure 2.3 [14]. It can be seen from the figure that the RSSI reading from CC2420 is very linear and has a dynamic range of about 100 dB.

The minimum LQI (`0x00`) and maximum LQI (`0xff`) values are associated with the lowest and highest quality compliant signals detectable by the receiver and LQI values

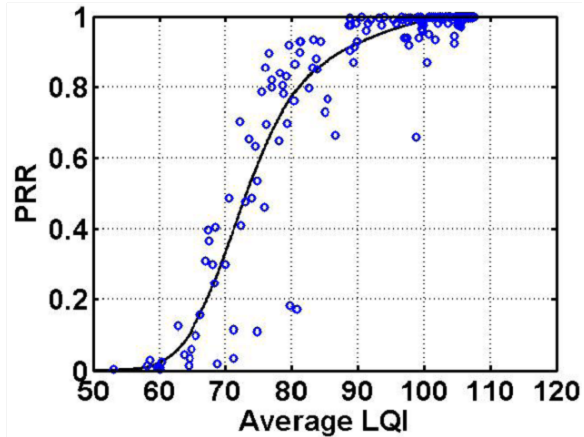


Figure 2.4: Correlation between Average LQI and PRR [12]

in between should be uniformly distributed between these two limits [3]. Software is responsible for generating the appropriate scaling of the LQI value for the given application. Using the RSSI value directly to calculate the LQI value has the disadvantage that e.g. a narrowband interferer inside the channel bandwidth will increase the LQI value although it actually reduces the true link quality. CC2420 therefore also provides an average correlation value for each incoming packet, based on the 8 first symbols following the SFD. This unsigned 7-bit value can be looked upon as a measurement of the "chip error rate," although CC2420 does not do chip decision. With the Frame check sequence, the average correlation value for the 8 first symbols is appended to each received frame together with the RSSI and CRC OK/not OK when MDMCTRL0.AUTOCRC is set. A correlation value of 110 indicates a maximum quality frame while a value of 50 is typically the lowest quality frames detectable by CC2420. Software must convert the correlation value to the range 0-255 defined by [3], e.g. by calculating: $LQI = (CORR - a) \times b$ limited to the range 0-255, where a and b are found empirically based on PER measurements as a function of

the correlation value. A combination of RSSI and correlation values may also be used to generate the LQI value. From [12], we can get information of the correlation between average LQI and PRR (Packet Reception Ratio) as Figure 2.4. If we look at the average LQI values marked by small circles in the middle of every horizontal line, it follows a rather smooth curve suggesting a better correlation with PRR.

In this thesis, the channels are classified with three categories based on the LQI values as clear channel (CC), available channel (AC), and interfered channels (IC) which are shown in Figure 2.5.

- Clear Channel: The sensors can communicate with its parent with low packet error rate. A clear channel is used for single channel communication in normal communication. The single channel is decided by the parent or collaboration with children.
- Available Channel: The sensors communicate with its parent under interference. There are packet drops or retransmissions depending on the channel quality.
- Interfered Channel: The sensors hardly communicate with its parent due to severe interference.

2.2 Adaptive Channel Hopping

2.2.1 Hopping Sequence Generation

The proposed Adaptive Channel Hopping algorithm utilizes a channel hopping sequence for coordination between the parent and child nodes of each group. The channel hopping sequence is periodically generated every $T_{LQIreport}$ seconds by the parent node and distributed to all child nodes via normal communication. Parent nodes generate this sequence first by gathering a Link Quality Information (LQI) map from each child node

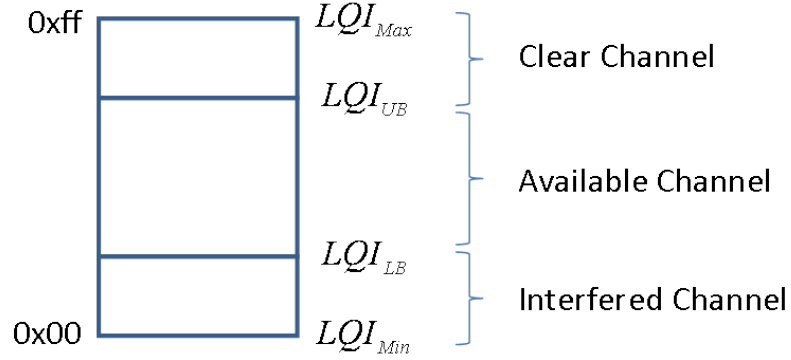


Figure 2.5: Channel Classification

which describes the current state of all N available frequency channels as shown in Figure 2.6. The complete LQI map gathered at the parent node contains LQI values represented as LQI_i^k , where i and k are the channel and node ids, respectively. For the current operating frequency, the LQI information can be estimated based on the Signal-to-Noise (SNR) ratio for recently received packets. For the remaining $N - 1$ frequency channels, nodes can act as an energy detector and estimate the current noise floor. To improve the accuracy of these readings, the child nodes scan the N frequency channels m times every $T_{LQIreport}$ seconds. An additional weighting factor, W^k , can be defined for each node k based on one of the following two scheme:

- Fair weighting: This method can be used as the default option in hopping sequence generation. If no weighting is required, all weighting factors are set to 1. ($W^k = 1$)
- Tree weighting: A sensor can be a relay node for the leaf nodes on the tree structure routing. The number of leaf tree node can be used for the weighting factor. ($W^k =$ number of leaf nodes)

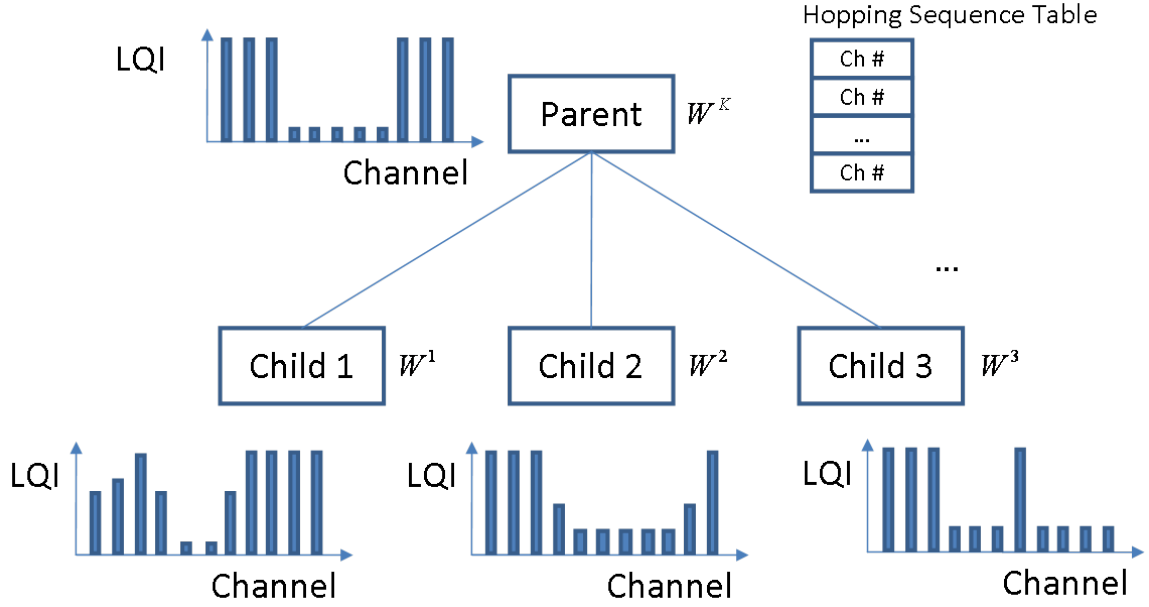


Figure 2.6: Hopping Sequence Generation

The nodes with a higher weighing factor will have a greater effect on the aggregate LQI (ALQI) calculation. The ALQI for each frequency channel can be calculated as shown in equation 2.1.

$$ALQI_i = \frac{\sum_{k=1}^K LQI_i^k W^k}{\sum_{k=1}^K W^k}, \quad (2.1)$$

where $i \in N$, K is the total number of group members. The channel hopping set is a list of available frequency channels, sorted by the calculated ALQI values. The channel with the highest ALQI value is the first channel in the channel hopping sequence. If no channel hopping sequence is available, such as during the initial stages of the network, by default the sensor network will scan the available frequency channels sequentially.

2.2.2 Channel Hopping Algorithms

Parent nodes utilizing the Adaptive Channel Hopping algorithm are assumed to have complete knowledge of the child nodes within their group. Coordination between the parent and child nodes is handled through a set of control messages as defined below:

1. Channel Hopping Command (CHC) message: CHC messages are transmitted by the parent. There are three usages of the message as follows:
 - The parent announces its existence on the operating channel by periodically sending command messages.
 - The parent sends a command to change an operating channel.
 - The parent sends a command to confirm a clear operating channel.
2. Channel Hopping Reply (CHR) message: CHR messages are transmitted by the children. There are two usages of the message as follows:
 - The children request channel hopping to the parent.
 - The children respond to the hopping command with the channel availability for the group.

When the parent detects interference sufficient to cause link quality degradation, loses communication with its child nodes for a pre-determined amount of time, or receives channel hopping requests from children, the sensor group tries to change its operating channel from the current operating frequency (f_c) to a newly selected frequency (f_n). The channel hopping scheme is Three-Way Handshake which includes the channel hopping command, reply of channel availability, and confirmation of channel use. The channel hopping algorithms for parent and children are as follows:

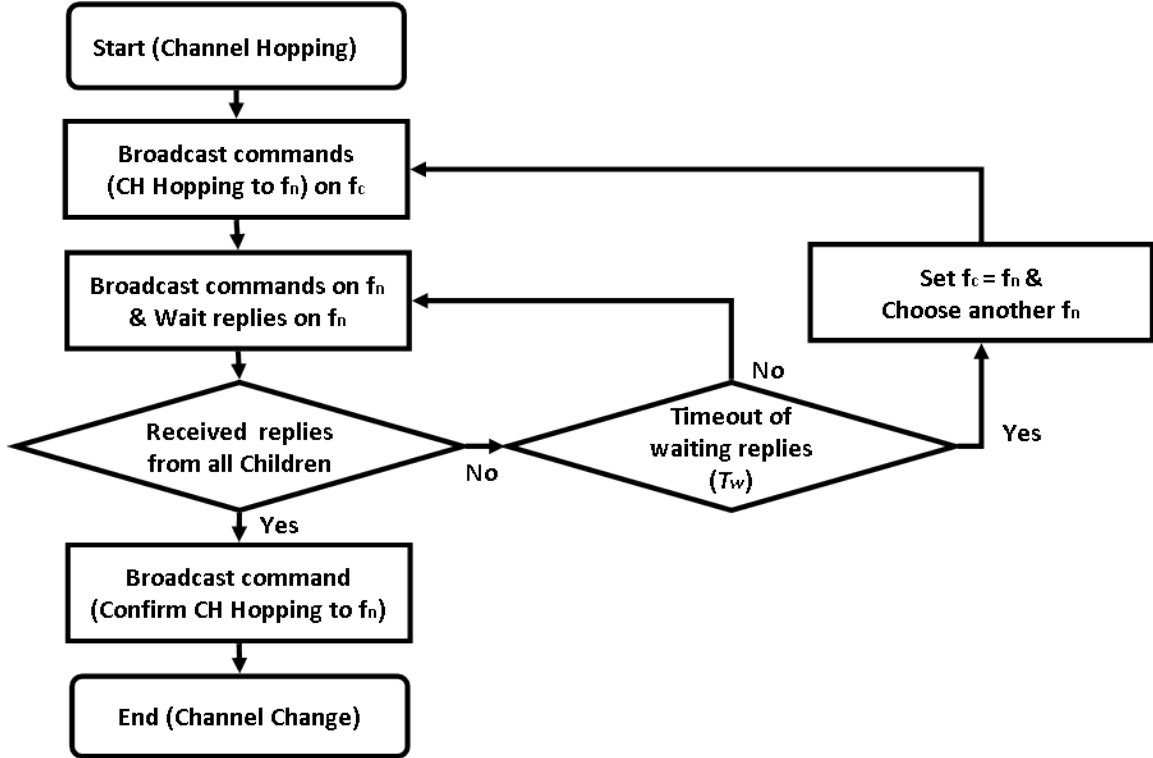


Figure 2.7: Channel Hopping Algorithm for Parent

The channel hopping algorithm for parent nodes is shown in Figure 2.7. When the operating channel is no longer available due to severe interference for more than the threshold time ($t_{LQI_i^k} < LQI_{LB} \geq t_{threshold}$, LB : Lower Bound) or the parent loses communication with its child nodes for threshold time, the parent broadcasts CHC messages on the current channel, f_c , to indicate a channel hop to the next channel in the channel hopping sequence, f_n . The CHC message is used to coordinate the channel hopping for all nodes within a group and is broadcasted b (default 3) times every T_M seconds. Upon hearing the CHC message, all child nodes reply with a CHR message on the new frequency, channel f_n . All

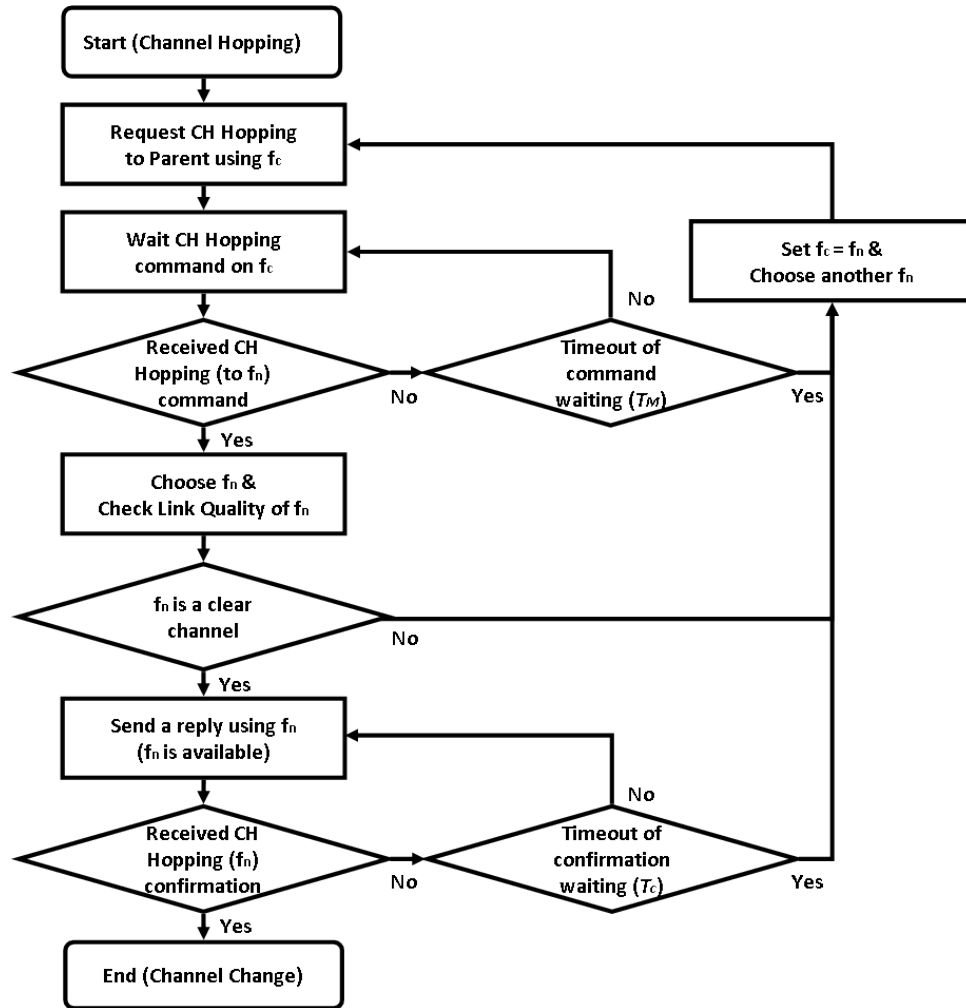


Figure 2.8: Channel Hopping Algorithm for Children

of these control messages are transmitted via a CSMA/CA mechanism. If the parent receives the CHR messages from all child nodes, it broadcasts confirmation CHC messages and then continues normal data communication. If the response from all children is not received after T_W seconds, it repeats the channel hopping mechanism with the next frequency channel in the pre-defined channel hopping sequence.

The channel hopping algorithm for child nodes is shown in Figure 2.8. When the child nodes detect severe interference for threshold time ($t_{LQI_i^k < LQI_{LB}} \geq t_{threshold}$), they transmit channel hopping requests to the parent. After transmitting this message, the child nodes wait for a pre-defined timeout period, $T_{Mb} = T_M \times b$. If a command message is not received within this timeout period, they continue scanning the frequency channels in the pre-defined channel hopping sequence described previously. When a child receives a channel hopping command from its parent node, and the LQI of the received packet is sufficient ($LQI_i^k \geq LQI_{LB}, UB : Upper Bound$), the child node responds to the parent with a CHR message. If a confirmation message is not received within T_C seconds the channel hopping sequence will continue. Due to the spatial distance between wireless nodes, it is possible that a child can experience severe interference, whereas the other nodes in the same group do not. Due to the circular nature of the channel hopping sequence, we can ensure that the parent and child will converge to either a new frequency channel that is clear of interference, or the same channel if the interference was temporary. The convergence of a group onto a single frequency channel is handled by carefully selecting the timeout values for channel switching.

For successful channel locking, the group should carefully choose the timeout values which are described as follows:

$$\begin{aligned} T_C &\geq (T_M + t_S) \times N, \\ T_W &\geq T_C \times 2 \geq (T_M + t_S) \times N \times 2, \end{aligned} \tag{2.2}$$

where t_S is channel switching time, and N is the number of channels to scan. For example, after a channel selection of a parent, the parent periodically (T_M) broadcasts command messages in the pre-determined time slot of the superframe. The children circularly and

incrementally scan the channels until they receive a channel hopping command. After receiving a channel hopping command and sending reply messages of the channel availability, they wait for a confirmation message from the parent. During the confirmation message wait time (T_C), the parent can collect replies from the other children. If the parent does not collect replies from all children after the waiting reply timeout (T_W), it then switches to the next channel in the channel hopping sequence. The *channel hopping latency* is defined as time from sending the first channel hopping command until all children receive a confirmation message. When the channel is locked at the K^{th} channel selection of the parent, the channel hopping latency is bounded as follows:

$$\begin{aligned}
K \cdot T_W + T_{Mb} &\geq L_{hopping} \geq (K - 1) \cdot T_W + T_{Mb} \\
&\geq (K - 1) \times T_C \times 2 + T_{Mb} \\
&\geq (K - 1) \times (T_M + t_S) \times N \times 2 + T_{Mb}.
\end{aligned} \tag{2.3}$$

Figure 2.9 shows an example of channel locking timing diagram after parent’s channel selection. After choosing channel n , the parent periodically broadcast command messages in the pre-determined time slot of the superframe. The children circularly (and incrementally in the example of Figure 2.9) scan the channels until they receive a channel hopping command. After receiving a channel hopping command and sending reply messages of the channel availability, they wait a confirmation message from the parent. During the confirmation message wait time, the parent can collect replies from the other children.

2.2.3 Packet Model and Channel Hopping Latency

The packet model of IEEE 802.15.4 sensor networks (shown in Figure 2.10) is proposed and mutual interference between IEEE 802.15.4 and IEEE 802.11b is analyzed in [10]. The parameters of the packet model are shown in Table 2.1. An average packet transmission delay of sensor networks is defined as the total time from the moment that a packet is located at the queue in a sender to the time to receive an ACK packet transmitted by the

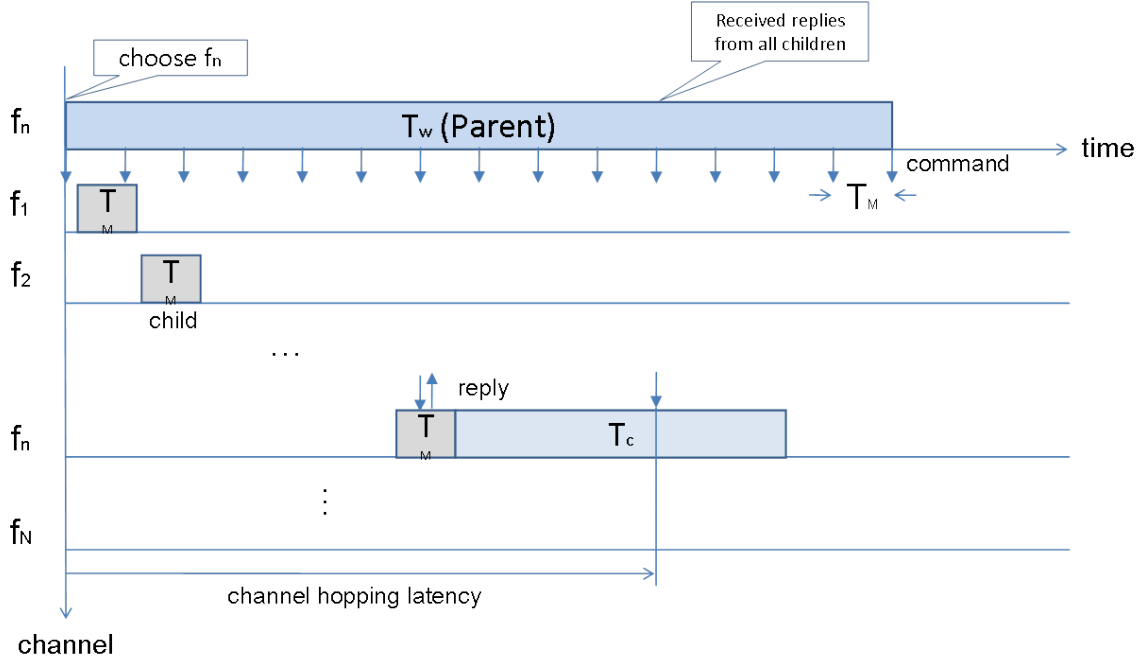


Figure 2.9: An Example of Channel Locking Timing Diagram

receiver. Then, the average packet transmission delay of sensor networks is obtained as

$$E[T] = t_f \sum_{i=0}^{\infty} iP^i(1 - P) + t_s = \frac{P}{1-P}t_f + t_s \quad (2.4)$$

, where P is a packet error rate, t_f and t_s are the time required for successful and unsuccessful transmission [10]. The t_s and t_f can be expressed as

$$\begin{aligned} t_s &= U_{backoff} + T_{CCA} + D + t_{TA} + T_{ACK}, \\ t_f &= U_{backoff} + T_{CCA} + D + t_{ackwait}. \end{aligned} \quad (2.5)$$

An example of the sensor network packet transmission is shown in Figure 2.11. A sensor node performs a random backoff and CCA, and transmits a packet but it fails in the example. Then the retransmission is successful with a packet transmission delay of T_R . Because of the interference, a desired packet needs to be retransmitted several times.

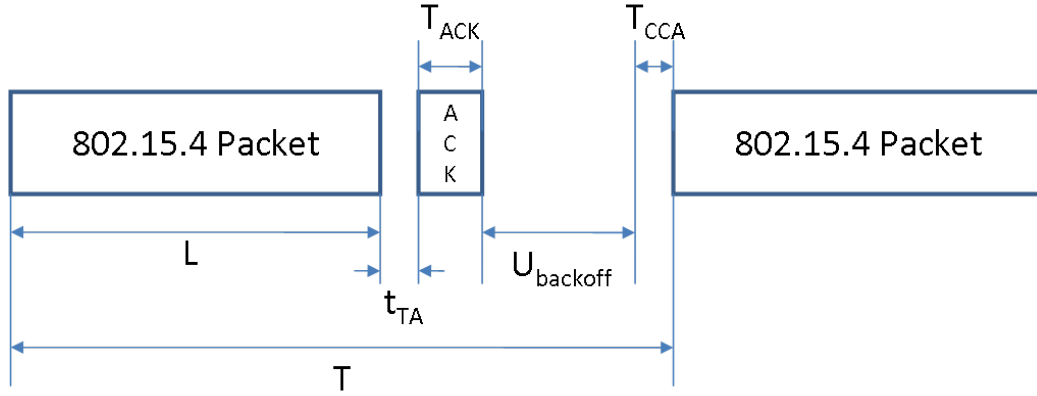


Figure 2.10: Packet Model of IEEE 802.15.4 Sensor Networks

The channel hopping latency, L , at the K^{th} channel selection of the parent can be expressed as

$$L = (K - 1) \times T_W + (n - 1) \times T_M + T_B \times 2 + T_{PR} + E[T] \times C + T_{PC} + T_{Mb}, \quad (2.6)$$

where n is the number of commands when the last child receives a command, C is the number of children who receive the command at the n^{th} command broadcasting, T_B is

Table 2.1: Parameters of the Packet Model

Parameter	Definition	Value
T_i	Inter-arrival time between 802.15.4 packets	varying
M	Duration of 802.15.4 packet	varying
t_{TA}	Turn-around time	$192\mu s \leq t_{TA} \leq 512\mu s$
T_{ACK}	Duration of 802.15.4 ACK packet	$352\mu s$
$t_{ackwait}$	Maximum wait duration for ACK packet	$864\mu s$
$U_{backoff}$	Average backoff time of 802.15.4	$1120\mu s$
T_{CCA}	Clear channel assessment (CCA) time	$640\mu s$

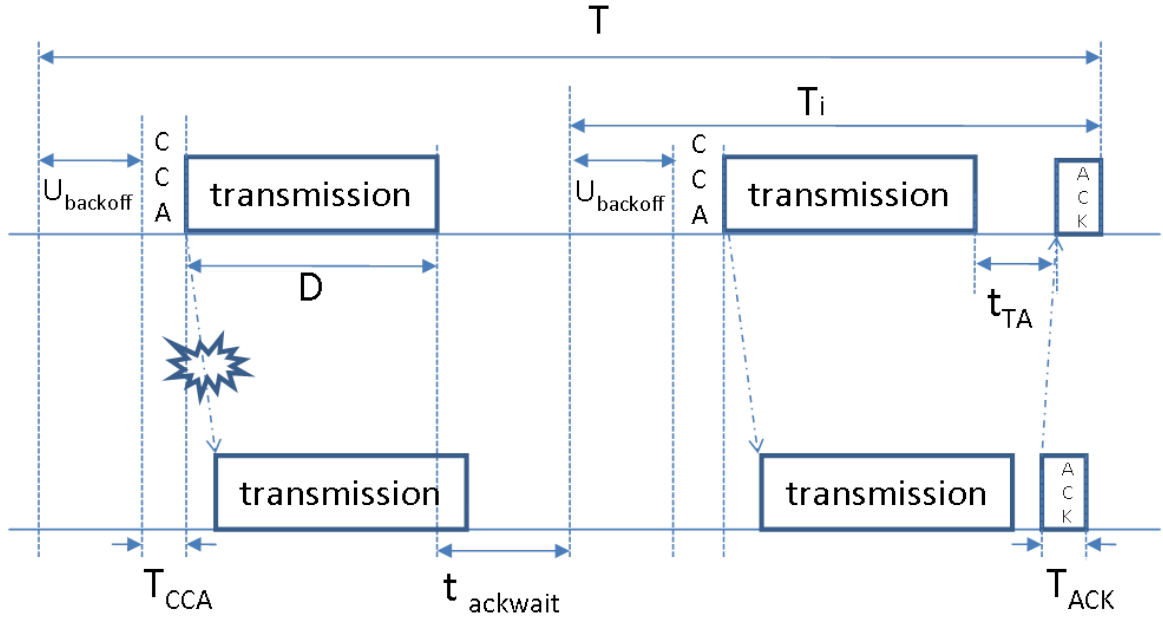


Figure 2.11: An Example of Transmission Delay

an average packet broadcasting delay, T_{PR} is processing time of a reply message, T_{PC} is processing time of a confirmation message.

2.3 Sensor Network Simulation and Results

2.3.1 Sensor Network Simulator

To simulate a sensor network utilizing the Adaptive Channel Hopping algorithm, we have developed a custom network model using the wireless sensor network simulator, Prowler [11] as shown in Figure 2.12. Prowler is an event-driven simulator that can be set to operate in either deterministic mode or in probabilistic mode. In the simulation, we use a radio propagation model which is frequently used model of the signal strength versus distance given by $P_{rec,ideal}(d) = P_{transmit} \frac{1}{1+d^\gamma}$, where $P_{rec,ideal}$ is the ideal reception signal

strength, $P_{transmit}$ is the transmission signal power, d is the distance between the transmitter and the receiver, and γ is a decay parameter with typical values of $2 \leq \gamma \leq 4$. When the application emits the send packet event, after a random wait time the MAC layer checks if the channel is idle. If not, it continues the channel status checking until the channel is idle with random backoff time. When the channel is idle, the transmission begins and the application receives the packet sent event after transmission time. After the reception of a packet on the receiver's side, the application receives a packet received or collided packet received event, depending on the success of the transmission [11].

In the following simulations, we model a single group consisting of one parent and 19 child nodes which all utilize the 802.15.4 protocol for communication. All nodes are within communication range of all other nodes. The processing time, T_{PR} and T_{PC} , were set to $192 \mu s$, the channel switching time, t_S , to $500 \mu s$, and the command interval T_M to 10 ms. Data and control packets are 120 and 40 bytes in length, respectively. The simulation was repeated 20 times to generate average results.

2.3.2 Channel Hopping Latency Measurement

First of all, we measure average channel hopping latency in converging on a free channel (error free channel) with the number of sensor nodes and the number of channels. The channel hopping is started by a channel hopping command message from the parent who decides operating frequency change. For the sake of pure channel hopping latency measurements in the first scenario, we set the group find a clear channel at the first channel selection ($K = 1$) because the latency is linearly dependent on the number of channel selection K . In the simulation with fixed K , two parameters n (the number of command messages when the last child receives a command at the channel selection) and C (the number of children

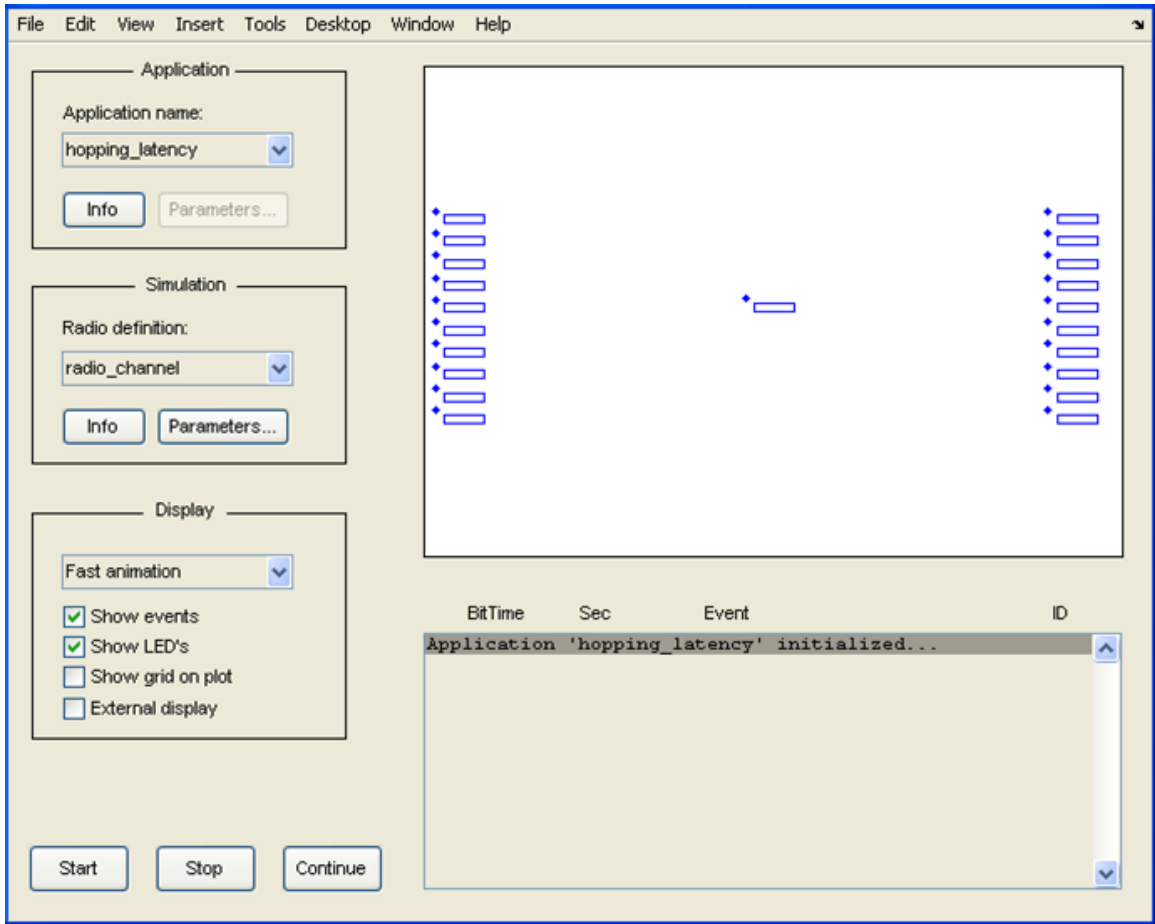


Figure 2.12: Wireless Network Simulator

who receive the command at the command broadcasting) are dominant on the measurement of hopping latency. In the first scenario to see the converging latency without the effect of n , we measure the channel hopping latency in case all children receive a command at the first broadcasting and report the channel is available. In Figure 2.13, channel hopping latency increases from 0.052 sec to 0.358 sec as the number of children increases from 1 to 20. Due to collision between sensor nodes and their backoff time, the latency curve shows smoothly increasing curve when the number of children increases. In case the number of

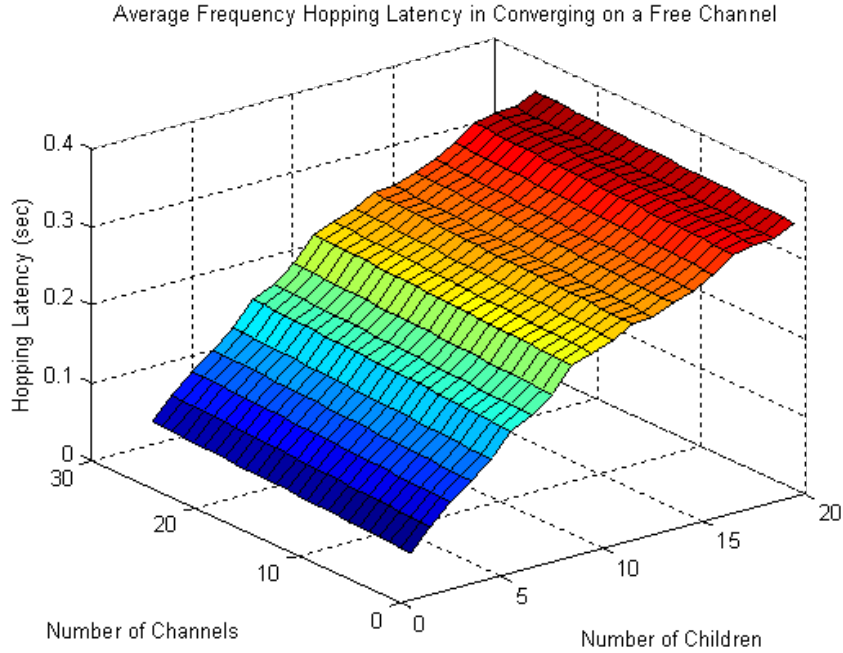


Figure 2.13: Channel Hopping Latency

channel number increase, the latency increases small amounts depending on the channel sensing delay.

In the channel hopping, children may receive a command message at different times due to their different timeouts or transmission errors. To see the effect of the number of commands in hopping latency, we define successful channel hopping command (CHC) message reception ratio of the children as P_C which is ranged from 0.05 to 0.95 and measure and calculate the channel hopping latency. The number of channels, N , is fixed at 27 which is half of the maximum number of command broadcasts in the proposed system. From the results of the second scenario in Figure 2.14, the channel hopping latency is ranged between 0.084 and 0.7625 sec. In the range of P_C decreasing from 1 to 0.4, the latency is slightly

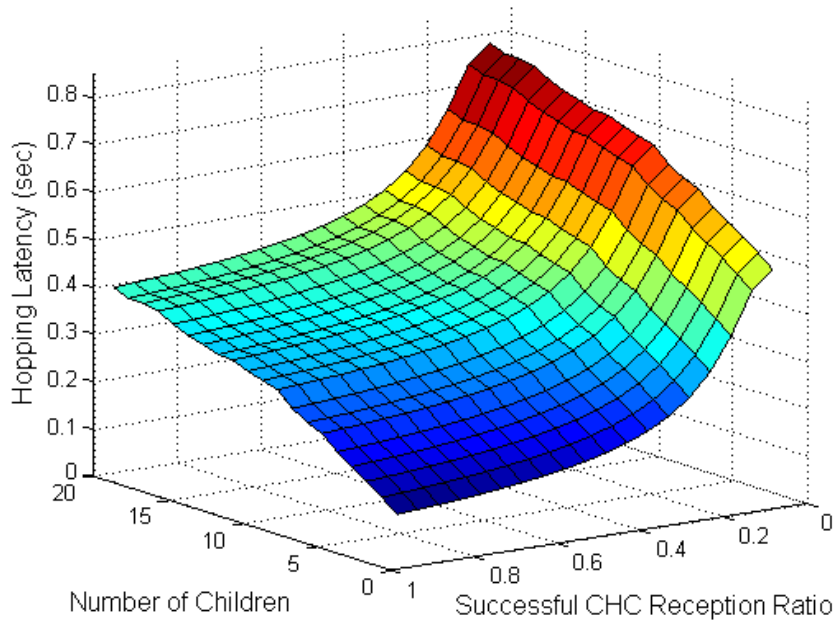


Figure 2.14: Channel Hopping Latency with Successful CHC Reception Ratio

increased, whereas there is rapid latency increase below 0.4 of P_C due to low possibility of command reception of the children. If the parent does not receive any reply message from the last group member after 54 command broadcasts ($T_W = (T_M + t_S) \times N \times 2 = 567ms$), the parent selects a new channel and broadcasts channel hopping command messages again. After channel locking fail on each channel selection, the latency increases 0.567 second at each channel selection.

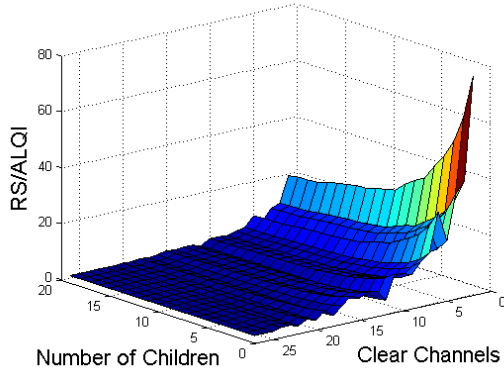
2.3.3 Channel Hopping Latency Comparisons

We proposed channel hopping sequence generation algorithm, ALQI, which can be used for channel ordering to minimize channel hopping latency and select an optimal channel. To evaluate our proposed scheme, we choose two channel selection algorithms as follows:

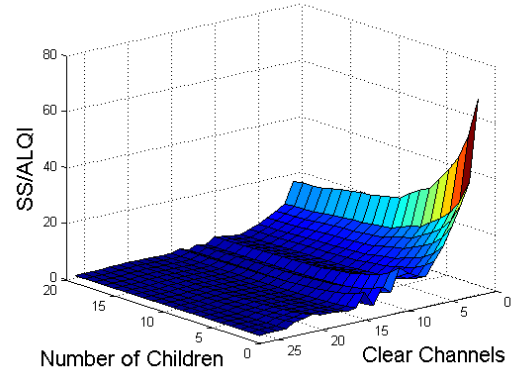
- Random Sequence (RS): The channel hopping sequence is randomly generated from the target channels.
- Sequential Sequence (SS): The channel hopping sequence is generated by sequentially and circularly increasing order from the current channel.

In the first comparison, the total number of channels is 27 in which a channel is used for current communication and 26 channels can be used for the channel hopping. Based on the correlation between LQI and PRR (packet reception ratio) [12], the channels with high LQI value are configured to have high PRR. In the comparison, we set the sensor group has the same clear channels which have high LQI values ($\geq LQI_{UB} = 100$ with $PRR \geq 0.95$) and are ranged from 2 to 27. The RS and SS are configured to have the same timeout mechanism as ALQI. In the comparison, average latencies of ALQI have similar as in previous measurements. In comparison of RS/ALQI and SS/ALQI, the ratios greater than 1 mean that ALQI has superior performance.

In comparison results in Figure 2.15, the ratios are greater than 1 in all ranges. We note that ALQI requires channel information sharing and sorting in normal situation which is not used in RS and SS. Despite the additional activities in normal communication, the latency is significantly reduced by the prompt channel locking at the channel switching. Without shared channel information, RS and SS consume large amounts of time for channel



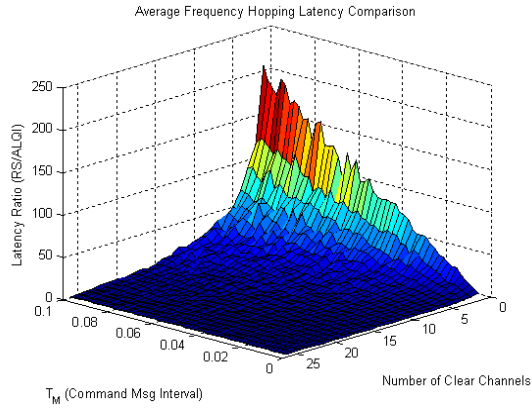
(a) Comparison of RS/ALQI



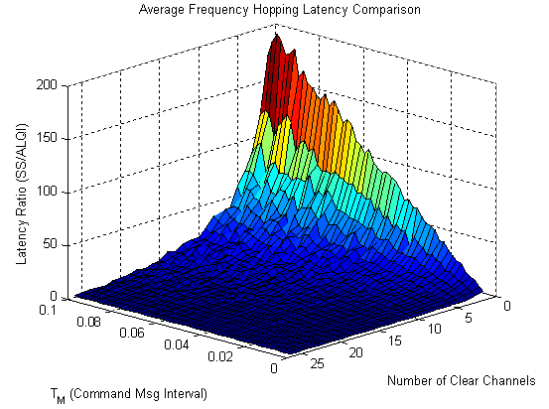
(b) Comparison of SS/ALQI

Figure 2.15: Channel Hopping Latency Comparison

locking and the largest latency of RS and SS is $14.772 \text{ sec} (T_W \times 26 + T_{Mb})$ if there is at least one clear channel among channel selection. The results in Figure 2.15(a) and 2.15(b) show ALQI has significant benefits on channel hopping latency in the range of the number clear channels between 1 and 20. This means the sensor group can have shorter channel hopping latency with ALQI in case more than 25% of channels are used. One channel of Wi-Fi consumes about 25% of the channels in 2.4GHz ISM bands. Thus, our proposed method will have great benefits in the coexistence with Wi-Fi. In case the number of clear channel is more than 20, ALQI has relatively small benefits because of high channel locking probability of RS and SS. Beyond the clear channel number of 20, the comparison ratios converge on 1 because there are enough clear channels. In the comparison with the number of children, ALQI significantly outperforms RS and SS as the number of children decreases because the latencies of ALQI are relatively shorter than total latencies of RS and SS.



(a) Comparison of RS/ALQI



(b) Comparison of SS/ALQI

Figure 2.16: Latency Comparison with Command Message Interval Change

In stead of the number of children, we provide a comparison with another parameter, the command message interval, which is an important parameter in the proposed system to minimize channel hopping latency. In this comparison, the number of children is fixed as 20. In comparison results with command message interval in Figure 2.16, the ratios are greater than 1 in all ranges and ALQI has great benefits in the range of low number of clear channels and command message interval with more than 5ms. In the range of short command message interval and high number of clear channels, ALQI has relatively small benefits in comparison of channel hopping latency. Because the interval of the command message decreases, the latencies of RS, SS, and ALQI are decreased together. But, there are limitations for reducing the interval such as high spectrum usage and power consumption. Furthermore the interval should be greater than channel switching time ($T_M \geq t_s$) and the average packet transmission delay of sensor nodes ($T_M \geq E[T]$) for reliable channel locking. In [10], average transmission delay ($E[T]$) of the IEEE 802.15.4 under IEEE 802.11b

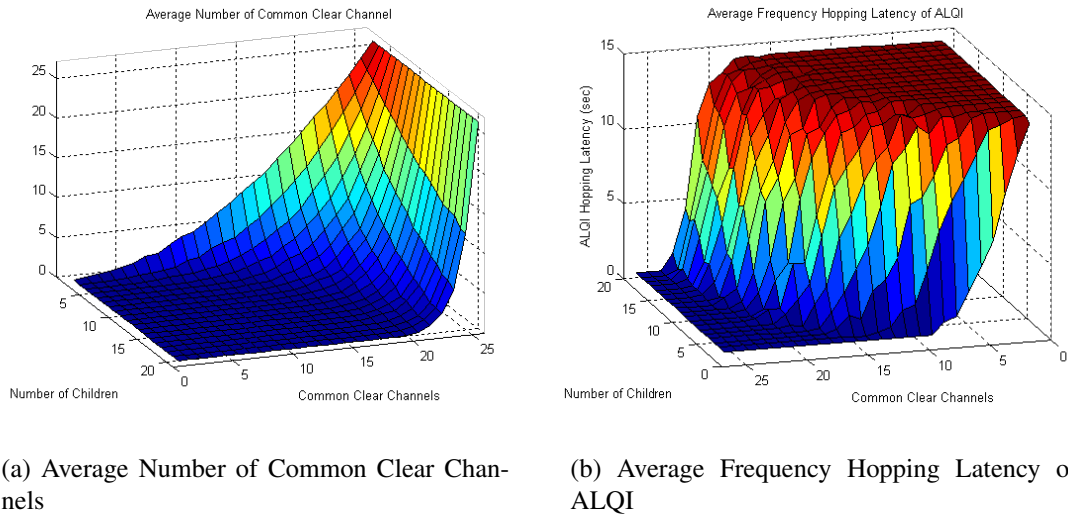
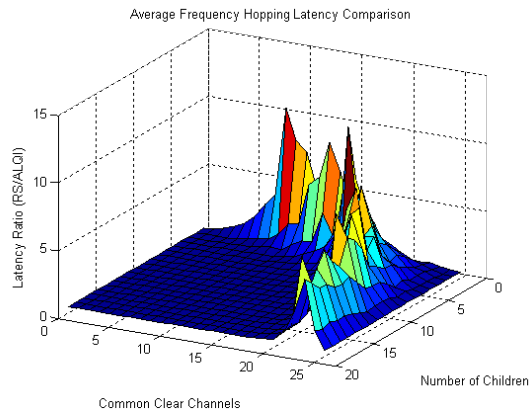


Figure 2.17: Common Clear Channel and Average Latency of ALQI

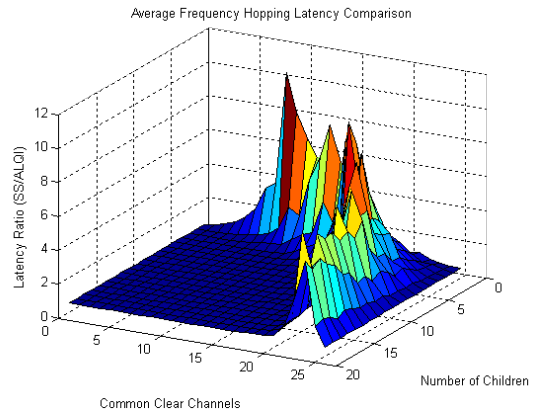
interference is greater than 6 ms in which range proposed ALQI has great performance benefits (short channel hopping latency). Overall, RS and SS show similar performance in latency comparisons.

2.3.4 Channel Hopping Latency Comparisons in Different Interference Levels

In real environments, sensor nodes might have different interference depending on their location. To see the difference levels of interference on each child, we configure each child has different interference on each channel. For a control parameter of channel environments, each child is configured to have the same number of clear channel though the clear channels might be in different frequency bands. When there is no common clear channel for the group members, the latency is configured to be 14.742 sec which is 26 rounds of channel selection and the comparison ratios are converged to 1. Figure 2.17(a) shows av-



(a) Latency Comparison of RS/ALQI

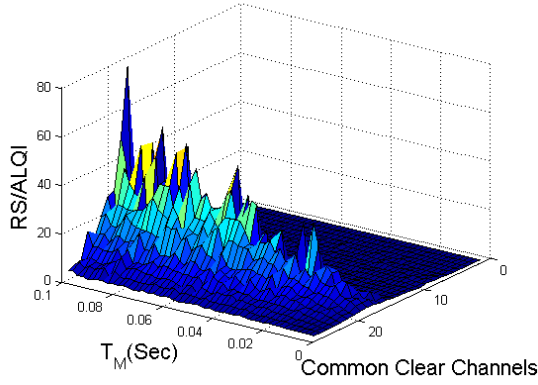


(b) Latency Comparison of SS/ALQI

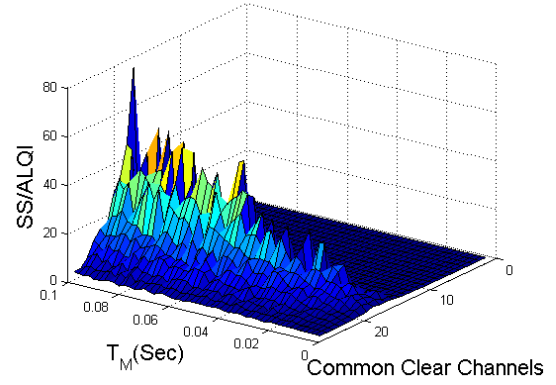
Figure 2.18: Latency Comparison with Different Levels of Interference

average number of common clear channels in the comparison. When the number of children is small, there are more chances of having common clear channels. In Figure 2.17(b), average frequency hopping latencies of ALQI are shown. When the group has at least one common clear channel, the latency is measured lower than 1 sec which area is bottom land of the result graph. But, if there is no common clear channel, the latencies are converged to 14.742 sec after 26 channel selections which is the top area of the graph.

With the same conditions in Figure 2.17, the comparisons of RS/ALQI and SS/ALQI are shown in Figure 2.18. When there is no common control channel or all channels are clear, the ratio is converged to 1 in the comparison. As long as the sensor group has at least one clear channel, ALQI has short channel hopping latency. In the Figure 2.18, ALQI is superior to RS and SS in the ranges between 20 and 25 of common clear channels and between 1 and 5 of children. The maximum benefit of ALQI over RS and SS is having about 10 times shorter latency with 10 ms of command message interval.



(a) RS/ALQI with T_M



(b) SS/ALQI with T_M

Figure 2.19: Latency Comparison with CM Interval and Different Interference Levels

In this comparison instead of the number of children, we use another parameter, the command message interval (T_M), which is an important parameter in the proposed system to minimize channel hopping latency. In the comparison, the number of children is fixed as 5. In the Figure 2.19, we can see similar comparison results as in Figure 2.16. As the command message interval increases, ALQI has more performance benefits. In the comparison ALQI has shorter channel hopping latency, as long as the sensor group has at least one clear channel among target channels. In this comparison, the maximum benefits are located around 17 common clear channels. The location of maximum benefit is dependent on the number of children due to the possibility of existence of common clear channels among children. When the number of children goes to small, the peak region will be located in smaller than 17 whereas when the number of children goes to high, the peak will be in larger than 17 of clear channel number. Overall, RS and SS show similar performance in latency comparisons.

Table 2.2: Throughput and Hopping Latency Comparisons

Throughput (Kbps)	Before Switching		Same levels of interference		Different levels of interference	
	PRR 0.95	PRR 0.35	Latency (Sec)	After hopping	Latency (Sec)	After hopping
ALQI	35.12	12.59	0.191	35.99	2.627	35.99
RS			0.436	35.98	7.251	35.81
SS			0.433	35.97	7.143	35.81

2.3.5 Throughput and Hopping Latency Comparisons

Finally, we compare the average rate of successful message delivery over communication channels. The throughput of wireless sensor networks, ρ , is defined as the total amount of packets received during a specific time at the destination. To compare overall throughputs (packets/second or Kbps) based on previous simulations, we choose common parameters as 27 total channels, 17 clear channels, 5 children, 10ms command message intervals, 0.95 and 0.35 of PRR before switching, a selection of common clear channel between 0.95 and 1 of PRR after switching. Table 2.2 shows the throughput and average channel hopping latency comparisons. Before channel switching, the throughputs are 35.12 Kbps with 0.95 PRR and 12.59 Kbps with 0.35 PRR. After the channel hopping is complete, each channel hopping mechanism converges to a channel with greater than 0.95 PRR. Due to the improved channel hopping sequence of the ALQI method, less time is required to find a new channel with both similar and different levels of interference. Also, in the case of different interference levels the ALQI method converges to a channel of better quality, which results in a slightly improved channel throughput.

CHAPTER 3

VOLUNTARY SPECTRUM HANDOFF

3.1 Cognitive Radio Networks

The wireless networks currently use a fixed spectrum assignment policy. There is a large variation in the utilization of the assigned spectrum due to geographical and temporal variations. The limited available spectrum and inefficiencies in its use motivate the idea of opportunistically accessing the underutilized portion of the spectrum. As seen in Figure 3.1, the Federal Communication Commissions (FCC) frequency allocation chart indicates multiple allocations over all of the frequency bands [16], which reinforces the scarcity mindset.

The idea of opportunistically utilizing the spectrum has motivated the genesis of a new networking paradigm, referred to as Dynamic Access Network (DAN) or Cognitive radios. Cognitive radios were designed with a view to utilize the 'white spaces', 'spectrum hole', or gaps within the transmissions. The main functions for cognitive radio networks can be summarized as follows:

- Spectrum Sensing: Detection of the unused portions of the spectrum and efficiently utilizing them without interfering with the current users.

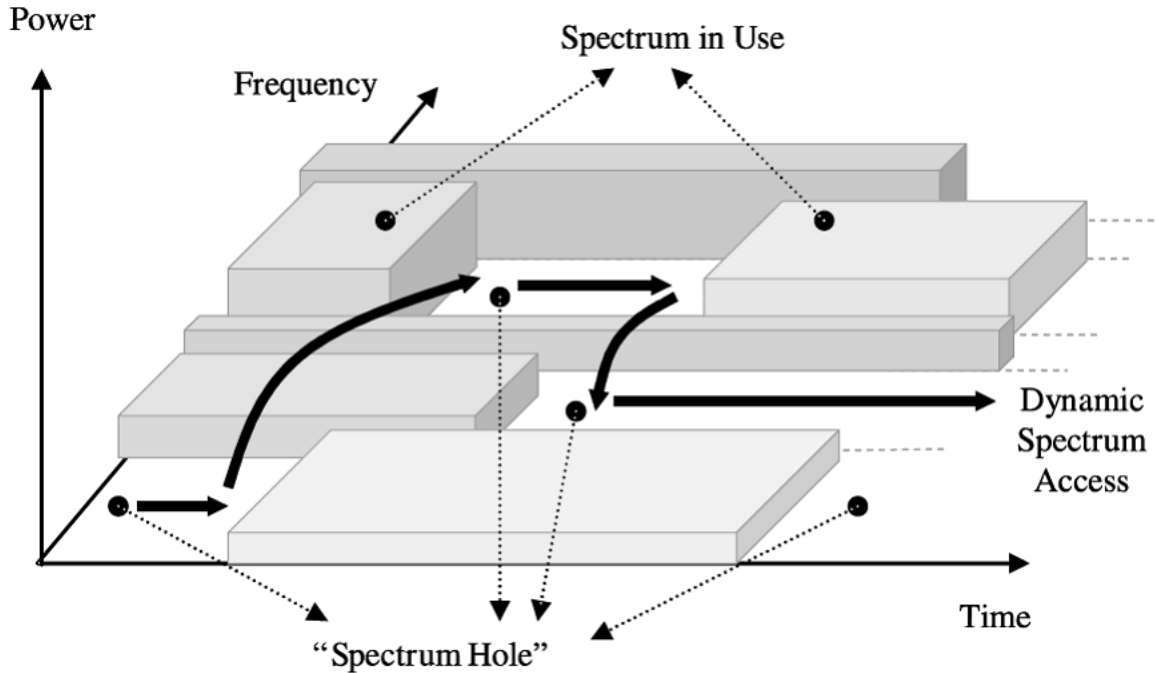


Figure 3.2: Cognitive Radio Concept [19]

Figure 3.2 [19]. The cognitive radio enables the usage of temporally unused spectrum, which is referred to as spectrum hole or white space. If this band is used by a licensed user, the cognitive radio moves to another spectrum hole or stays in the same band, altering its transmission power level or modulation scheme to avoid interference.

3.2 Architecture

In this thesis, to reduce communication disruption time which is caused by spectrum handoffs, we propose a new type of spectrum handoff referred to as *Voluntary Spectrum Handoff* (VSH) which is not triggered by the primary user detection. With the estimation of primary user spectrum usage, SUs estimate future PU presence and voluntarily change the spectrum without disruption to PUs. For the spectrum usage estimation of PUs, we

define two kinds of spectrum sensing period such as a fixed spectrum sensing window and a variable history window. To select an optimal spectrum which is currently unused and has the longest spectrum lifetime from the VSH time, we propose spectrum selection algorithms including spectrum lifetime estimation with primary user spectrum usage.

3.2.1 Assumptions

Our proposed work is based on the following assumptions about the underlying CRN:

- The model of “commons” is assumed for the CRN operation, which refers to the existence of secondary (unlicensed) users that use the licensed spectrum opportunistically and without disrupting primary (licensed) users’ operation.
- SUs are equipped with identical antennas which can be tuned to any one of N channels [19, 24].
- PU channel occupancy is modeled as an ON-OFF process alternating between ON (busy) and OFF (idle) periods [24, 25]. For the sake of clarity, we will focus on exponential and Erlang distributed ON-OFF periods. However, our methods can be applied to arbitrary ON-OFF period distributions using pdf estimation methods described in [30].
- There exists a dedicated common control channel for spectrum information sharing and communication channel setup [25, 27, 28, 29].
- To differentiate the channel usage of PUs and SUs, there is a spectrum log server which stores SUs’ channel usage [31, 32]. SUs and the spectrum server can directly communicate with each other.

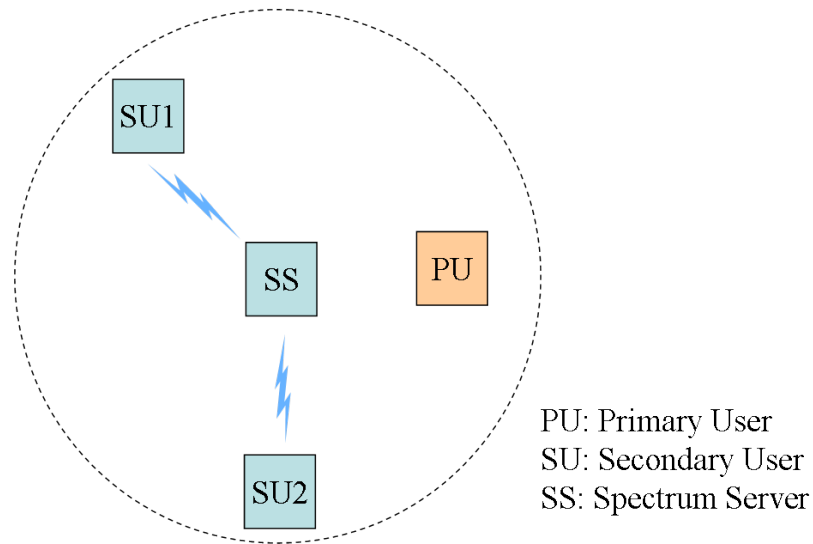


Figure 3.3: Network Model

3.2.2 Network Model

The proposed network architecture is composed of three types of devices as shown in Figure 3.3. PUs operate on licensed band and are “owners” of the band. SUs can sense spectrum and utilize unused licensed spectrum. SUs vacate licensed spectrum as soon as PU activity starts. SUs can operate on N licensed channels. To predict future PU activity, it is necessary to calculate past spectrum usage of PUs. The Spectrum Server (SS) is a log server which has the functionality of communicating with SUs over the common control channel. SUs record their spectrum usage with time information at the SS. The main functionalities of the SS are to store spectrum usage information of SUs and to provide spectrum information to other SUs upon request.

When an SU senses the spectrum locally, it observes the combined spectrum usage information of both PUs and SUs as shown in Figure 3.4. Spectrum usage of SUs is highly

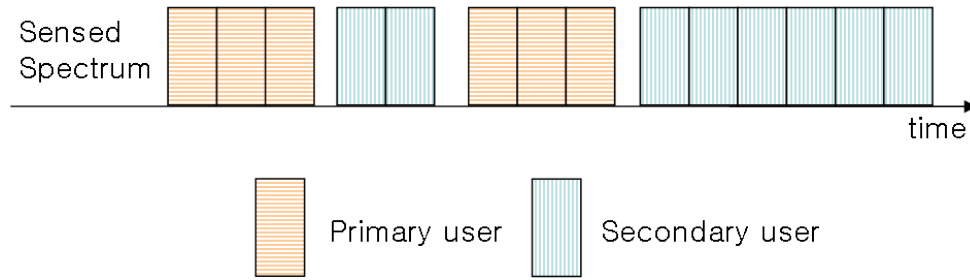


Figure 3.4: Spectrum Usages

dependent on PU spectrum usage because SUs can use the spectrum only when there is no active PU on a given channel. With the SU information provided by the SS, an SU can estimate the spectrum usage of PUs as the difference between the locally sensed combined usage and the information provided by the SS. We use a common control channel to exchange spectrum information with the spectrum log server and setup a communication channel with a correspondent SU.

3.3 Spectrum Usage Estimation

The estimation of PU spectrum usage in CRNs is an important step to decide on spectrum selection for the voluntary spectrum handoff procedures. Depending on the spectrum usage behavior of PUs, different estimation methods can be more accurate. When the PU traffic is more dynamic and fast varying as in cellular networks, spectrum estimation mechanisms should be more adaptive to reflect the traffic behaviors. Even when PU traffic behavior is statistically steady, PU spectrum usage may dynamically change whenever the SU moves to new locations. To cope with spectrum usage behavior changes, we define two sensing periods: sensing window and history window. Sensing window is the basic

time unit over which spectrum usage is observed. An SU takes S samples of a channel's status during a sensing window T . Each sample is converted to a binary value representing primary user activity or non-activity. SUs compute PU spectrum usage as the difference between the locally sampled binary values and the binary values of SU spectrum usage provided by the SS. The average obtained during a sensing window represents a short term statistics of the PU usage. A short term observation obtained in a sensing window gives statistics that are generally valid locally, but that may have deviated from a longer term average. For estimations to be useful for VSH, statistics must be averaged over longer periods of time. When PU usage process does not vary over time, longer periods of observation yield better estimations. Therefore, we use a history window of length K , $K \geq T$, for estimation purposes. The value of K is increased as long as the average estimated in a sensing window does not deviate more than ϵ fraction of the average obtained over the history window. If the deviation is more than ϵ , then K is decreased aggressively to capture changes that occur in the PU spectrum usage behavior.

3.3.1 Sensing Window Size Selection

We assume that changes in the PU behavior occur over periods of time in the order of several minutes, and the channel usage parameters remain steady over a given sensing window. The basic step of spectrum usage estimation is to decide on the sensing window size. Since an SU does not know the traffic behavior or rates of PUs, the spectrum sensing window size must be inferred from the spectrum sensing data. We introduce one possible decision rule of minimum spectrum sensing window size. The spectrum usage can be represented by the sequence of busy (used) state "1" and idle (unused) state "0" [24, 25]. In the On-Off channel model, the sojourn time of an ON period for channel n is modeled

as a random variable T_{ON}^n with the probability density function $f_{T_{ON}^n}(y)$, $y > 0$. Similarly, an OFF period is modeled as T_{OFF}^n with $f_{T_{OFF}^n}(x)$, $x > 0$ [24]. The observation is based on the cycles of the spectrum states. We define a spectrum cycle C as the time from the beginning of one state to the end of another state. For example, a cycle starts at the start time of “1” state and lasts until the end time of subsequent “0” state. The average of l spectrum cycles C_l^n on channel n is computed as follows:

$$C_l^n = \sum_{k=1}^l \frac{\sum_{t=m_{k-1}+1}^{m_{k-1}+m_k} X^n[t]}{m_k} / l, \quad m = \sum_{k=1}^l m_k \geq 2l \quad (3.1)$$

where $X^n[t]$ is the binary channel observation obtained in channel n at t , m_k ($m_0=0$) is the number of samples on the k^{th} spectrum cycle, and m is the number of total samples. With the spectrum cycle average, the sensing window size can be chosen such that the following inequality holds:

$$var(C_l^n) \leq \alpha, \quad l \geq l_{min} \quad (3.2)$$

In Equation 3.2, the spectrum cycle count l should be no less than a minimum number of spectrum cycles, l_{min} . According to the PU spectrum usage in real world, we can estimate general probability density function using the observed sample data or pdf estimation method in [30]. The general distribution can be applied to our system model. In this thesis, for the sake of clarity we introduce two example distributions including exponentially distributed On-Off model with the pdf of

$$\begin{aligned} f_{T_{OFF}^n}(x; \lambda_{T_{OFF}^n}) &= \lambda_{T_{OFF}^n} e^{-\lambda_{T_{OFF}^n} x}, \\ f_{T_{ON}^n}(y; \lambda_{T_{ON}^n}) &= \lambda_{T_{ON}^n} e^{-\lambda_{T_{ON}^n} y} (x, y > 0) \end{aligned} \quad (3.3)$$

and Erlang-distributed On-Off model with the pdf of

$$\begin{aligned} f_{T_{OFF}^n}(x; k, \lambda_{T_{OFF}^n}) &= \frac{\lambda_{T_{OFF}^n}^k x^{k-1} e^{-\lambda_{T_{OFF}^n} x}}{(k-1)!}, \\ f_{T_{ON}^n}(y; k, \lambda_{T_{ON}^n}) &= \frac{\lambda_{T_{ON}^n}^k y^{k-1} e^{-\lambda_{T_{ON}^n} y}}{(k-1)!} (x, y > 0). \end{aligned} \quad (3.4)$$

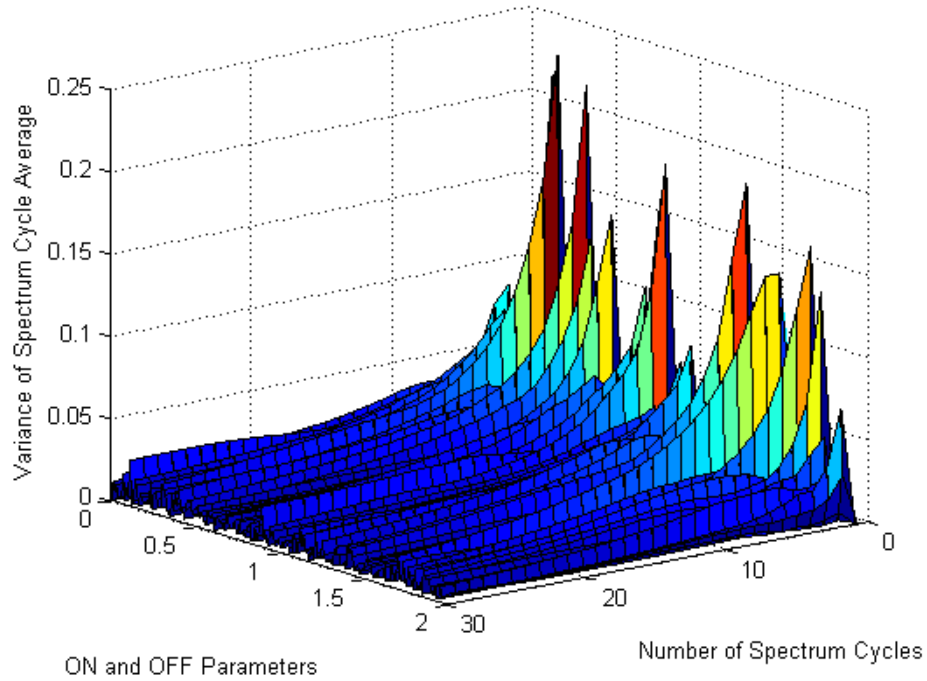


Figure 3.5: Spectrum Cycle Average Variance

From the example of exponentially distributed On-Off processes, we can see stable spectrum usage estimation results with the number of spectrum cycles which are decided by the tuning parameter $\alpha=0.05$ and the minimum cycle count $l_{min}=10$. This estimation model can be extended to arbitrary distributions using methods described in [30] as well. To see the effects of the variance of spectrum cycle average on the sensing window, we measure the variance traces with spectrum cycle lengths ranging from 1 to 30, and with λ_{ON} and λ_{OFF} rates ranging from 0.01 to 2.0. Figure 3.5 shows the measurement results of spectrum cycle average variances. From the graph, the variances converge below 0.05 after around 15 spectrum cycles, which means that the sensing average will be stable and the minimum sensing window size can be chosen from this spectrum sensing cycle. The results are also

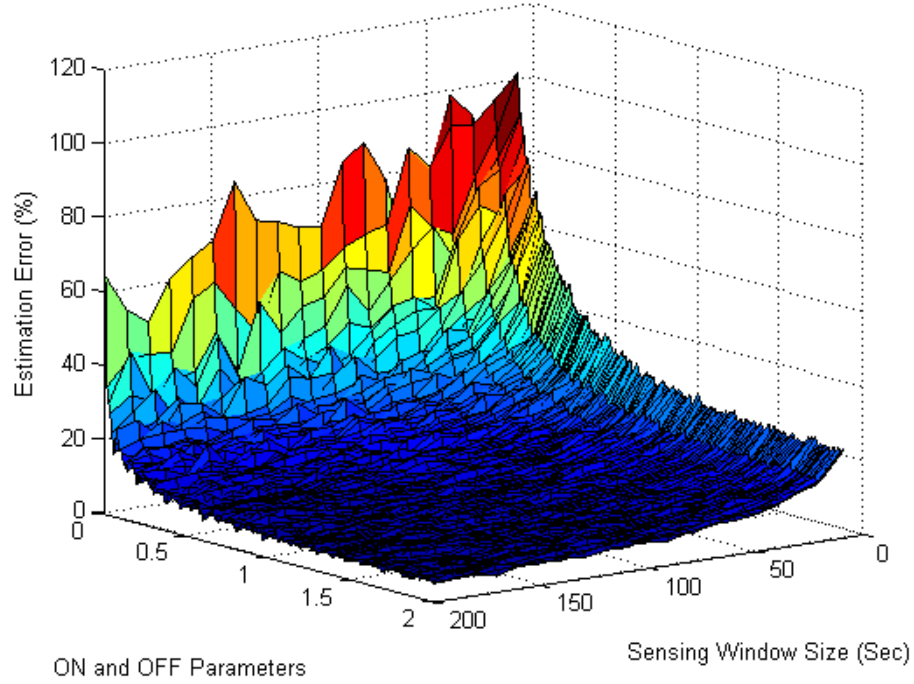


Figure 3.6: Estimation Error with Sensing Window

effective for Erlang distribution. In general case, if we know the spectrum cycle number l with any distribution of T_{ON} and T_{OFF} , we can obtain the spectrum sensing time T^n for channel n as follows:

$$T^n = l \times [E\{T_{ON}^n\} + E\{T_{OFF}^n\}] \quad (3.5)$$

To see the actual estimation error, we measure estimation errors with changing sensing window sizes between 10 and 200 seconds and with equal λ_{ON} and λ_{OFF} rate parameters between 0.01 and 2.0 in Erlang distribution with $k=2$. The estimation error after m sampling, $m \geq T^n$, is calculated as

$$\frac{|(\sum_{t=1}^m X^n[t])/m - (\sum_{t=1}^{T^n} X^n[t])/T^n|}{(\sum_{t=1}^m X^n[t])/m} \times 100 \quad (3.6)$$

From the results graph shown in Figure 3.6, we observe that the estimation errors converge as sensing window size increases except for very low λ_{ON} and λ_{OFF} rates. In case of low rates, estimation errors are still decreasing with larger sensing window size. If the sensing window size is chosen larger than 200 in case ON and OFF parameters are no smaller than 0.5, the estimation error will be no more than 5%.

3.3.2 Spectrum Usage Estimator

To estimate PU spectrum usage with history window, we introduce a spectrum usage estimator which is implemented in the MAC layer. The input of the spectrum usage estimator is spectrum sensing data that already excludes the spectrum usage of SUs. To get PU only spectrum usage information, an SU requests SUs' spectrum usage information from SS every T period. Until receiving SU spectrum usage information from SS, the SU assumes current channels are used only by PUs. Every sensing time, the spectrum usage estimator calculates PU spectrum usage ratio with history window data. The history window size is increased by one or decreased by D fraction of history window with the deviation criterion ϵ in Equation 3.8. The estimated average in general case on channel n at time t (assumed as an integer) can be expressed as follows:

$$\frac{\overline{X_{T^n}}}{\overline{X_{K^n}}} = \frac{\frac{1}{T^n} \sum_{i=1}^{T^n} X^n[t - T^n + i]}{\frac{1}{K^n} \sum_{i=1}^{K^n} X^n[t - K^n + i]} \quad (3.7)$$

History window size K on channel n is computed using Equation 3.8:

$$K^n = \begin{cases} \min(K^n + 1, K_{MAX}^n), & \text{if } \frac{|\overline{X_{K^n}} - \overline{X_{T^n}}|}{\overline{X_{K^n}}} \leq \epsilon \\ \max(\lfloor K^n - D \times K^n \rfloor, T^n), & \text{otherwise} \end{cases} \quad (3.8)$$

To demonstrate the accuracy of the spectrum usage tracking, we compare our proposed history window schemes with the fixed spectrum sensing window case. The spectrum sensing window is set to 200 seconds. We choose the maximum history window size as ten times

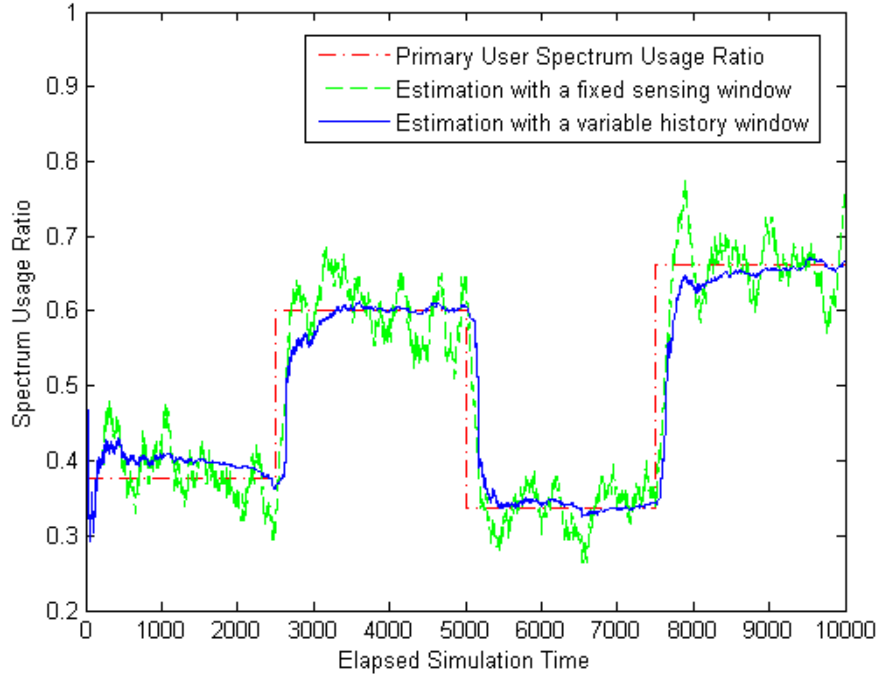


Figure 3.7: Primary User Spectrum Usage Estimation

of the sensing window size. In this model, we consider one channel and the SU estimates the PU spectrum usage. To check comparison results from two traffic distribution examples, we choose PU traffic source to be exponentially distributed with $E\{T_{ON}\}=0.8$ and $E\{T_{OFF}\}=1.25$ in $0 < t \leq 2500$, and $E\{T_{ON}\}=1.25$ and $E\{T_{OFF}\}=0.8$ in $2501 \leq t \leq 5000$; and Erlang-distributed ($k = 2$) with $E\{T_{ON}\}=0.5$ and $E\{T_{OFF}\}=1.0$ in $5001 \leq t \leq 7500$, and $E\{T_{ON}\}=1.0$ and $E\{T_{OFF}\}=0.5$ in $7501 \leq t \leq 10000$. To decide on spectrum environment changes, we use the coefficient $\epsilon=0.2$. We choose a reduction ratio of $D=0.2$. From Figure 3.7, we can see that the proposed history window scheme has better tracking performance with smaller fluctuations on spectrum usage ratio estimation, $(\sum_{t=1}^m X[t])/m$, where m is the sample size, when compared with a fixed sensing window of 200.

3.4 Spectrum Handoff Management

3.4.1 Voluntary Spectrum Handoff

In addition to conventional forced spectrum handoff, we define a new type of spectrum handoff, i.e., voluntary spectrum handoff. Voluntary spectrum handoff is triggered by reaching the threshold probability or time of PU presence prediction. Without PU detection, SU can predict a future presence of a PU and change the spectrum band which has lower probability of PU detection. The voluntary spectrum handoff time which is called *residual spectrum lifetime* can be estimated by the spectrum selection algorithms. The purpose of VSH is to reduce communication disruption time caused by the sudden PU presence. If an SU knows the time to switch to another channel, it prepares for channel switching by searching for spectrum holes and sharing spectrum information with other SUs in advance. In CRNs, the delay of FSH includes spectrum hole searching delay (t_{search}), spectrum information sharing delay ($t_{sharing}$) among SUs, channel ordering and selection delay ($t_{decision}$), and channel switching delay ($t_{switching}$). When a pre-prepared spectrum information is used with VSH, an SU can overlap the spectrum analysis and sharing time with the ongoing communication. Consequently, the actual communication of the SU continues while preparing for VSH. As a direct result, the communication session is disrupted for shorter periods of time under VSH than under FSH. The session disruption duration for FSH (D_{FSH}) and VSH (D_{VSH}) are expressed as follows:

$$\begin{aligned} D_{FSH} &= t_{search} + t_{sharing} + t_{decision} + t_{switching} \\ D_{VSH} &= t_{switching} \end{aligned} \quad (3.9)$$

3.4.2 Spectrum Lifetime Estimation

When an SU predicts PU presence (or end of the spectrum lifetime) by probabilistic calculations through PU spectrum usage estimation, it switches to a new spectrum band

without detecting a PU. The spectrum lifetimes of target channels for VSH are estimated by two algorithms. The proposed algorithms are based on the probability derived from the probability density function which is estimated from the averages ($E\{T_{ON}^n\}$ and $E\{T_{OFF}^n\}$) and variances ($var(T_{ON}^n)$ and $var(T_{OFF}^n)$) of ON and OFF periods on the channel sensing data. For the general type of pdf which is not formulated by the average and variance, we can adopt a pdf estimation method such as [30]. The proposed two algorithms are as follows:

TPS (Transition Probability Selection)

In CRNs, the derivations of transition probabilities for the general ON/OFF processes using Laplace transform are introduced in [24]. For example, the transitions probabilities for exponentially distributed ON/OFF periods can be expressed as follows:

$$\begin{aligned} P_{00}^n(t) &= (1 - u^n) + u^n \times e^{-(\lambda_{ON}^n + \lambda_{OFF}^n)t} \\ P_{01}^n(t) &= u^n - u^n \times e^{-(\lambda_{ON}^n + \lambda_{OFF}^n)t}, \\ u^n &= \frac{\lambda_{OFF}^n}{\lambda_{ON}^n + \lambda_{OFF}^n} \end{aligned} \quad (3.10)$$

Likewise, the transitions probabilities for Erlang-distributed ($k=2$) ON/OFF periods can be expressed as follows:

$$\begin{aligned} P_{00}^n(t) &= 1 - \frac{1}{4} \frac{(\lambda_{ON}^n - \lambda_{OFF}^n)^2}{\lambda_{ON}^n} e^{-\frac{1}{2}(\lambda_{ON}^n + \lambda_{OFF}^n)t} \frac{\sinh(\frac{1}{2}Ct)}{C} \\ &\quad + \frac{1}{4} [-4\lambda_{ON}^n \lambda_{OFF}^n - (\lambda_{ON}^n - \lambda_{OFF}^n)^2 e^{-(\lambda_{ON}^n + \lambda_{OFF}^n)t} \\ &\quad + (\lambda_{ON}^n + \lambda_{OFF}^n)^2 e^{-\frac{1}{2}(\lambda_{ON}^n + \lambda_{OFF}^n)t} \cosh(\frac{1}{2}Ct)] (1 - u^n) \\ P_{01}^n(t) &= 1 - P_{00}^n(t), \\ C &= \sqrt{(\lambda_{ON}^n)^2 - 6\lambda_{ON}^n \lambda_{OFF}^n + (\lambda_{OFF}^n)^2} \end{aligned} \quad (3.11)$$

With the transition probabilities P_{00} (state transition probability from idle state to idle state) and P_{01} (state transition probability from idle state to busy state) from renewal theory, we can estimate spectrum lifetime for VSH. We define the spectrum lifetime t_n on channel n with transition probabilities as follows:

$$t_n = \operatorname{argmax}_{0 < t \leq (t_{Max} - K^n)} \{t | P_{00}^n(t) \geq P_{01}^n(t)\} \quad (3.12)$$

In the TPS algorithm, there are two extreme cases depending on the distributions of PU spectrum usage. The first case is that the probability crossover does not happen due to low PU activities. In this case, SU will stay on the same channel and change spectrum via forced spectrum handoff. The second case is that a short spectrum lifetime is estimated such as “ $0 < t_n \leq \text{one sensing period}$ ”. In this case, the spectrum lifetime t_n is set to one sensing period and SU switches to a new channel due to the prediction of imminent PU presence only if there are channels with longer spectrum lifetime estimation.

RBS (Reliability Based Selection)

RBS based on the reliability theory [33] and estimates spectrum lifetime of the OFF periods. To derive a general equation, we define the following; T : time until next primary user detection (r.v.), t : time after the detection of no primary user, $S(t)$: spectrum lifetime function, $F(t)$: cumulative distribution function of T , $f(t)$: probability density function of T . Spectrum lifetime function can be defined as follows:

$$S(t) = P(T > t) = 1 - P(T \leq t) = 1 - F(t) \quad (3.13)$$

The spectrum lifetime function $S(t)$ is a curve describing the proportion of spectrum availability by time t and expressed in terms of cumulative distribution function $F(t)$ which can be an arbitrary distribution describing the off process. Primary user detection rate $\mu(t)$ is defined as the relative rate for spectrum lifetime function decline:

$$\mu(t) = -\frac{dS(t)}{S(t)dt} = -\frac{d}{dt} \ln S(t) \quad (3.14)$$

From Equation 3.14, we can get general expression of spectrum lifetime function as follows:

$$S(t) = e^{-\int_0^t \mu(u)du} \quad (3.15)$$

For example, when T_{OFF}^n is exponentially distributed with rate λ_{OFF}^n , the detection rate can be replaced by constant rate.

$$\mu(t) = -\frac{S'(t)}{S(t)} = \lambda_{OFF}^n = const \quad (3.16)$$

With the constant primary user detection rate, the spectrum lifetime function can be described by the exponential function:

$$S(t) = e^{-\lambda_{OFF}^n t} \quad (3.17)$$

Likewise when T_{OFF}^n is Erlang-distributed, the detection rate can be expressed as following:

$$\mu(t) = \frac{(\lambda_{OFF}^n)^k t^{k-1} / (k-1)!}{\sum_{m=0}^{k-1} (\lambda_{OFF}^n)^m t^m / m!} \quad (3.18)$$

With the spectrum lifetime function, the spectrum lifetime t_n on channel n can be computed as follows:

$$t_n = \underset{0 < t \leq (t_{Max} - K^n)}{\operatorname{argmax}} \{t | S(t) \geq S_{threshold}\} \quad (3.19)$$

According to the spectrum lifetime, we can decide on a voluntary spectrum handoff time and select a new channel which has the longest residual spectrum lifetime. With the change of $S_{threshold}$ in RBS, we can control the activity of voluntary spectrum handoffs.

3.4.3 Voluntary Spectrum Handoff Process

Under VSH, an SU uses spectrum lifetime estimation to select a potential channel to switch to. The SU selects a channel which has the longest spectrum lifetime t_n that is estimated by the proposed algorithms. Before the spectrum selection, the unused spectrum information between SUs should be shared and negotiated over the common control channel. The sequences of events leading to a VSH are as follows:

1. Share the unused spectrum information and estimated spectrum lifetimes t_n between SUs
2. Decide on a channel which has the maximum spectrum lifetime on both SUs
3. Share and confirm the decision results
4. When spectrum lifetime expires, switch to the new channel

Note that steps 1~3 occur without disrupting the communication session of the SU under VSH. If a PU is detected before estimated spectrum lifetime, these steps are repeated (as in FSH) in which case all 4 steps contribute to the disruption duration.

3.5 Performance Evaluation

To evaluate our proposed schemes, we simulate voluntary spectrum handoff performance. For the basic simulation model, we assume N channels and an On-Off PU traffic source model. We assume that On-periods and Off-periods are iid positive random variables which have exponential or Erlang distributions. The simulation can be extended to various traffic distributions which are estimated from real spectrum sensing data. For the spectrum usage estimation and PU detection, SU senses all N channels every second. When an SU detects PU presence, it should vacate current spectrum without further transmission and search for a new empty spectrum band to continue its communication. For the forced spectrum handoff, we choose two spectrum selection algorithms as follows:

- Random Selection (RS): When FSH is triggered by PU detection, an SU randomly selects a channel among spectrum bands currently unused by PU.
- Lowest Average Selection (LAS): When FSH is triggered, an SU selects a channel which has the lowest average of spectrum usage on history window and currently

unused by PU. LAS is the same channel selection algorithm as choosing a channel with the lowest combined BTR presented in [25].

To evaluate our proposed schemes, we compare TPS and RBS ($S_{threshold}=0.5$) algorithms for VSH with RS and LAS for FSH. SUs switch to channels that are not occupied by PUs when handoffs occur. In our simulations, we count the numbers of forced and voluntary spectrum handoffs and measure the Communication Disruption Ratio (CDR). CDR is calculated as *disruption periods/total communication time*. In our simulations, the disruption period of SU communication increases in the following two cases:

- When FSHs or VSHs are triggered.
- When all channels are used by PUs.

If all channels are used by PUs, then the SU waits until a spectrum hole emerges. Simulation results about the channel switching and packet transmission delays are provided in several existing works [24, 25, 34]. In our system model, the delay components of FSH include t_{search} , $t_{sharing}$, $t_{decision}$, and $t_{switching}$. In [24], the channel switching delay including t_{search} , $t_{decision}$, and $t_{switching}$ is reported between 80 msec and 350 msec. In [34], the packet delay of a single hop communication is reported as 100 msec, which can be considered as $t_{sharing}/2$. With these simulation results, we assume that an SU's communication is disrupted for $D_{FSH}=500$ msec during FSH to detect spectrum holes and connect to another SU. In case of VSH, we assume that SU's communication is disrupted for 50 msec to switch to a new spectrum. In the simulation model, we choose a maximum history window size of 1000 sec, which is five times larger than the spectrum sensing window of 200 sec for all channels. The total simulation time is 5000 seconds for each configuration.

3.5.1 Spectrum Handoff Count Comparison

For various communication scenarios, we define 4 traffic patterns with Erlang distribution ($k=2$) which have different channel usage parameters as shown in Table 3.1. In Table 3.1, Identical Mode (IM) represents channel usage ratios on all channels are the same. Dense Mode (DM) represents high spectrum usage and Sparse Mode (SM) represents low spectrum usage. Hybrid Mode (HM) includes 3 different hybrid channels. In each mode, the number of channels is 9.

Table 3.1: Traffic Source Parameters

Parameters	IM	DM	SM	HM
$E\{T_{ON}\}$	3.0	9.0	3.0	3.0,6.0,9.0
$E\{T_{OFF}\}$	3.0	3.0	9.0	9.0,6.0,3.0

We summarize and compare spectrum handoff counts after 5000 seconds simulation time in Table 3.2.

Table 3.2: Spectrum Handoff Counts

Spectrum Handoff		IM	DM	SM	HM
RS	FSH	974	948	384	455
LAS	FSH	950	960	347	351
TPS	FSH	732	55	359	362
	VSH	947	3396	0	18
RBS	FSH	627	489	319	313
	VSH	1598	1699	299	343

In case of RS and LAS, we count only FSHs because there is no VSH. In identical mode, the VSH schemes including TPS and RBS have 23%~35% less FSHs and RBS has the lowest FSH counts as 627. In dense mode, both TPS and RBS reduce FSH counts significantly. In case of RS and LAS, the total FSH counts are 948 and 960 respectively. But, TPS can reduce the FSH counts to 55 with 3396 VSHs, and RBS can reduce the FSH counts to 489 with 1699 VSHs. In sparse mode, TPS and RBS have similar FSH counts as RS and LAS. In case of low PU spectrum usage, TPS and RBS cannot significantly reduce the FSH counts with VSH events. In hybrid mode case, RBS again has the lowest FSH counts. The FSH counts are sorted as $RBS < LAS < TPS < RS$. In all these simulations, it is evident that VSH schemes with TPS and RBS reduce forced handoffs and add more voluntary handoff events. We note that the total number of handoffs, both voluntary and forced, is larger under the two VSH schemes than under FSH schemes. Despite this increase, the communication disruptions are reduced as shown in Section V.B.

With the same simulation results of spectrum handoff count comparison, we compare the communication disruption ratio depending on the time changes. In the comparison graphs, the results have a transient effect during the first 1000 seconds of the simulations.

Identical Mode: In identical mode, all 9 channels are configured with Erlang distributed ON/OFF processes ($k=2$) with $E\{T_{ON}\} = 3.0$ and $E\{T_{OFF}\} = 3.0$ to simulate spectrum behavior in which ON and OFF rates are equal. In this traffic model, the PU spectrum usage ratio is around 50%. In Figure 3.8, while VSH schemes have around 10% disruption ratios and FSH methods have around 13% disruption ratios over total simulation time. This means that during 5000 seconds simulation time TPS and RBS with VSH have 150 seconds longer uninterrupted connection time which is caused by 23%~35% fewer FSHs shown in

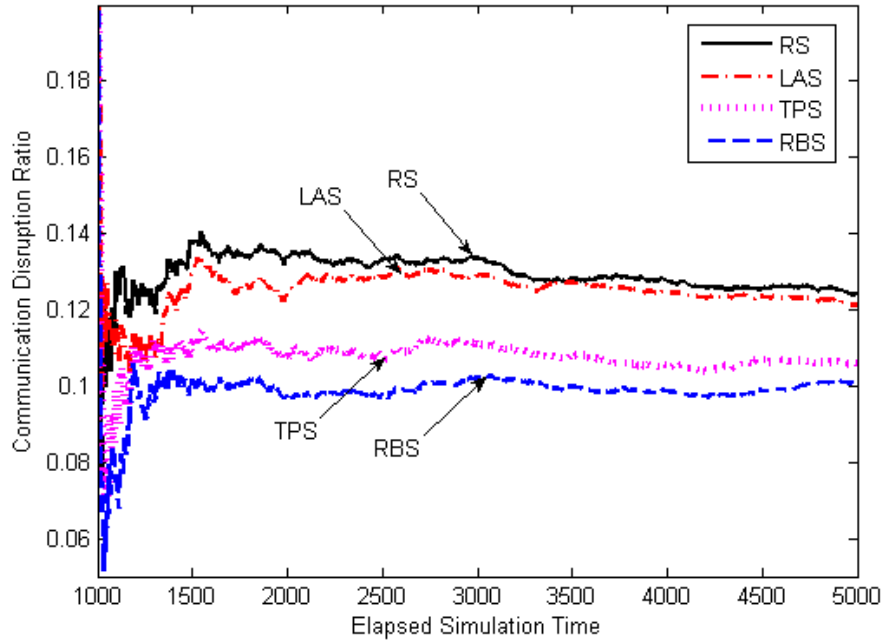


Figure 3.8: CDR Comparison for IM

Table 3.2. After 5000 seconds simulation, the performance is ordered as $RBS > TPS > RS > LAS$.

Dense Mode: In dense mode, all 9 channels are configured with $E\{T_{ON}\} = 9.0$ and $E\{T_{OFF}\} = 3.0$ to simulate high spectrum usage behavior. In this traffic model, the PU spectrum usage ratio is around 75%. From Figure 3.9, we can see the TPS and RBS have 11.5% and 14.5% disruption ratios respectively whereas RS and LAS have 19% disruption ratios. The 4.5%~7.5% performance gains of TPS and RBS are obtained from reducing FSH counts and replacing them with VSHs as shown in Table 3.2. This means that SUs can have longer uninterrupted connection times with VSH when PU spectrum usage ratio

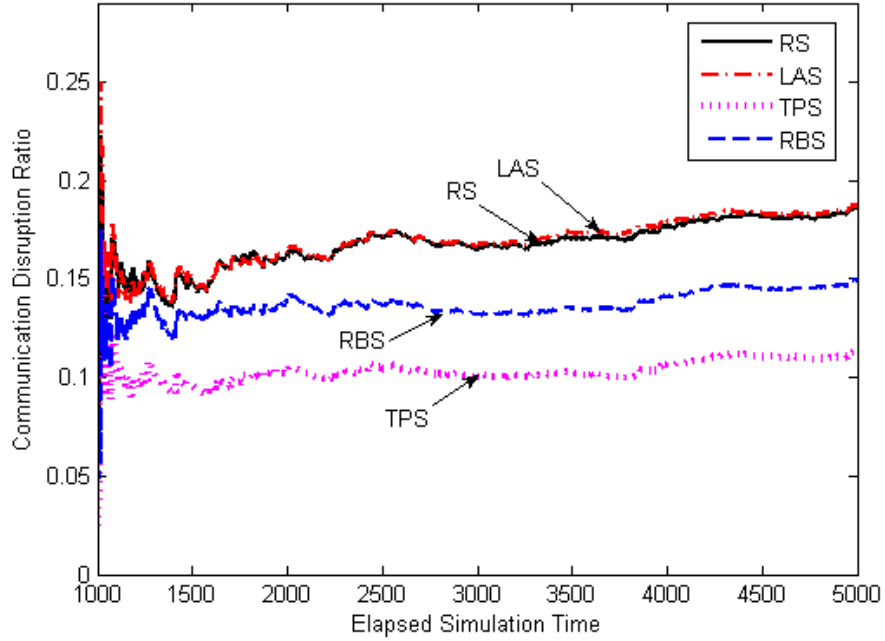


Figure 3.9: CDR Comparison for DM

is high. In comparison of each VSH schemes, TPS has superior performance from more aggressive VSHs than RBS. The performance is ordered as $TPS > RBS > LAS > RS$.

Sparse Mode: In sparse mode, all 9 channels are configured with $E\{T_{ON}\} = 3.0$ and $E\{T_{OFF}\} = 9.0$ to simulate low spectrum usage behavior. In this traffic model, the PU spectrum usage ratio is around 25%. From Figure 3.10, all spectrum selection algorithms including VSH schemes have similar disruption ratios around 4.3%~4.8%. This means the TPS and RBS schemes deliver small benefits since FSH occurs before estimated spectrum lifetimes are reached due to low PU spectrum usage.

Hybrid Mode: To simulate heterogeneous spectrum usage behaviors, 3 channels are configured with $E\{T_{ON}\} = 3.0$ and $E\{T_{OFF}\} = 9.0$, 3 channels with $E\{T_{ON}\} = 6.0$ and

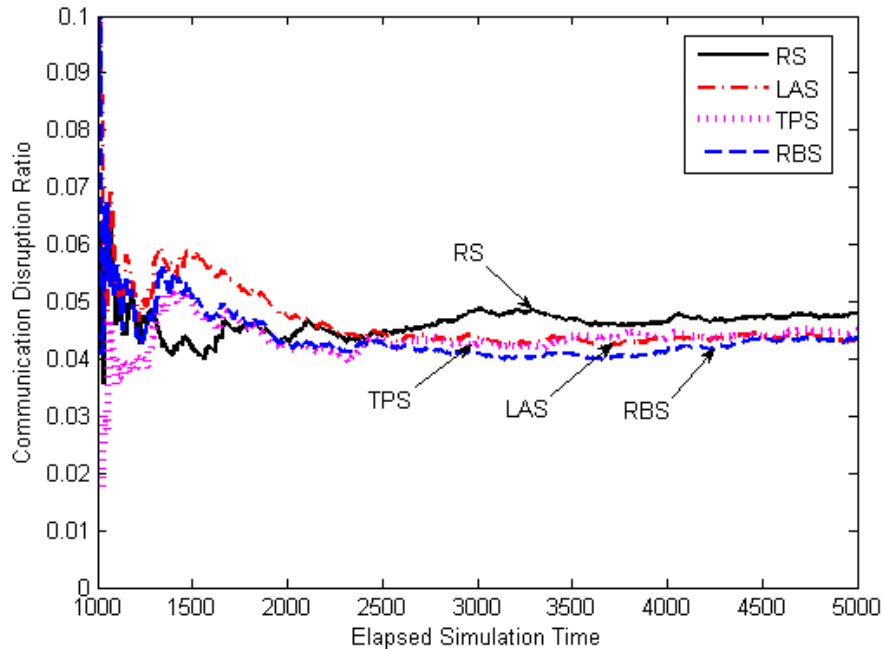


Figure 3.10: CDR Comparison for SM

$E\{T_{OFF}\} = 6.0$, and 3 channels with $E\{T_{ON}\} = 9.0$ and $E\{T_{OFF}\} = 3.0$. In this traffic model, the PU spectrum usage ratio is around 50% on average. In comparison results shown in Figure 3.11, LAS, TPS, and RBS have lower CDR than RS. The performance is ordered as $RBS > LAS > TPS > RS$. The sequences are the same as the reverse order of the forced spectrum handoff counts shown in Section V.A.

3.5.2 Communication Disruption Ratio Comparison

3.5.3 Effect of Primary User Spectrum Usage

To show the effect of PU spectrum usage, we ran another set of simulations where PU spectrum usage ratios are varied between 0 (no channel is used by PUs) and 1 (all channels are used by PUs) with exponentially distributed On-Off periods. The PU spectrum usage

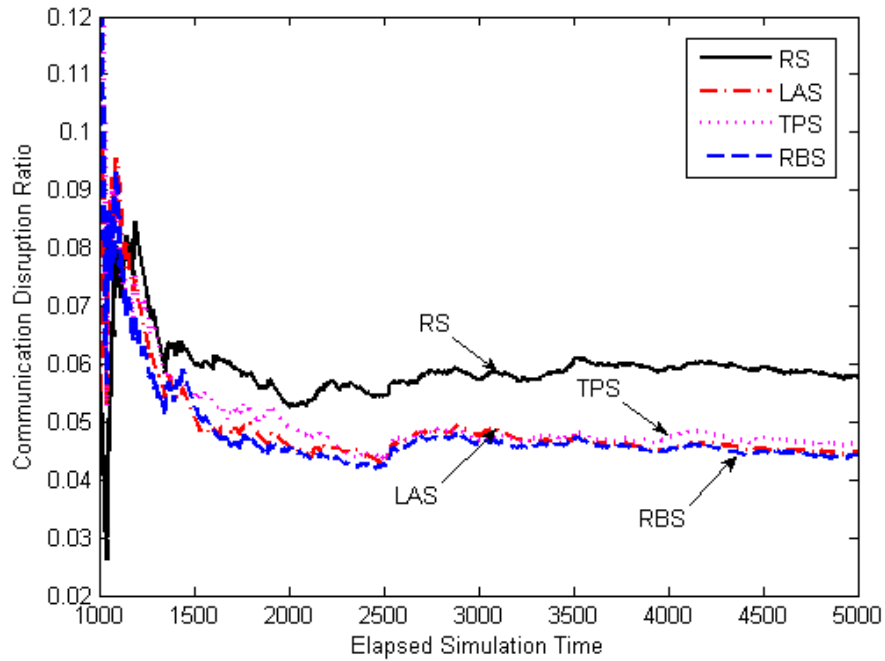


Figure 3.11: CDR Comparison for HM

ratio on a channel n is defined as $E\{T_{ON}^n\}/(E\{T_{ON}^n\} + E\{T_{OFF}^n\})$ which is varied from 0 to 1 on each 9 channels. In every parameter combination, we average the results for 5000 seconds simulation time.

For CDR comparisons of all spectrum selection algorithms with different PU spectrum usages, the control of PU spectrum usage ratios is achieved using a variable $\lambda_{ON}=1/E\{T_{ON}\}$ and a fixed $\lambda_{OFF}=1/E\{T_{OFF}\}$ as 1/3. Figure 3.12 is the extended version of Figure 3.8 with different probability density function (from Erlang to Exponential) and various PU spectrum usage ratios (from a fixed ratio of 0.5 to variable ratios between 0 and 1). Figure 3.12 shows that TPS and RBS have lower disruption ratios in most cases. Between 0.3 and 0.9 of PU spectrum ratio, VSH schemes have benefits from voluntary handoffs by

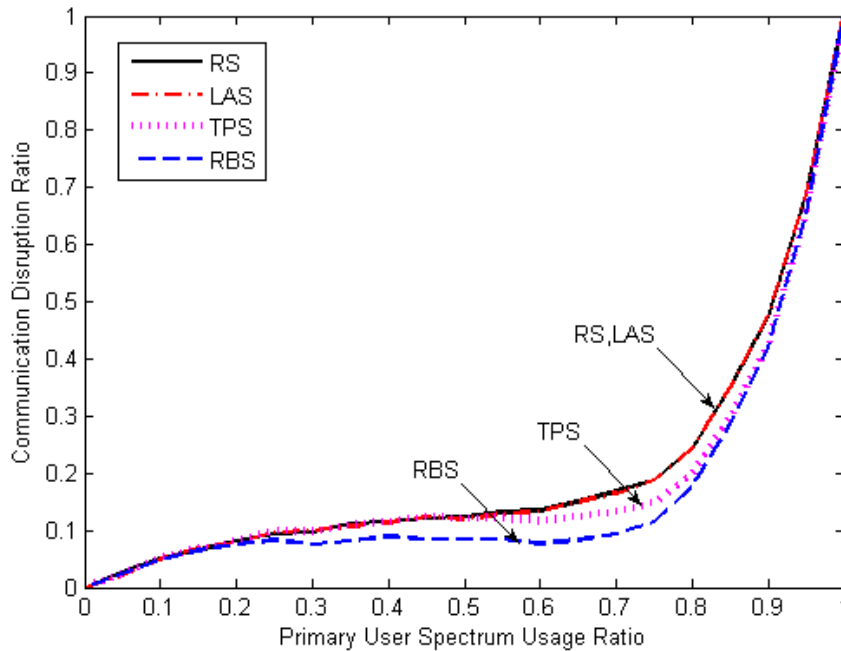
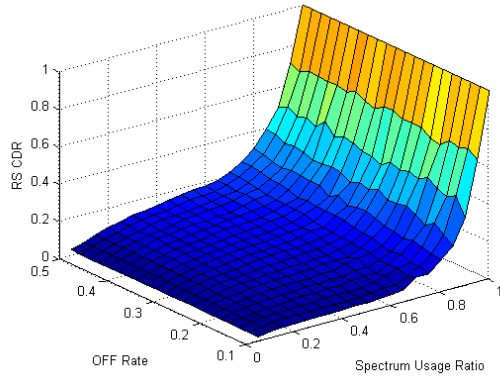


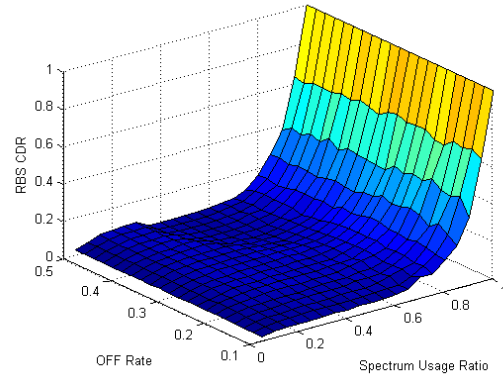
Figure 3.12: CDR Comparison with $E\{T_{OFF}\} = 3$

reducing forced handoffs. Between VSH schemes, RBS has better performance in most cases. Between 0.3 and 0.8 of PU spectrum ratio, RBS quite aggressively reduces FSH counts with active VSHs and has lower disruption ratios than TPS VSH scheme. The aggressive VSHs of RBS are caused by short spectrum lifetime estimation. Beyond PU spectrum ratio of 0.8, all VSH schemes show similar behaviors which indicates that they estimate spectrum lifetimes similarly. The sharp increase in CDR between 0.8 and 1 is caused by the unavailability of available channels in the network with increased PU activity.

To see the effects of various traffic parameters, we measure each CDR with variable λ_{ON} and λ_{OFF} and compare CDR ratios based on the RBS CDR. Figure 3.13(a) and



(a) RS CDR with Various Traffic Parameters



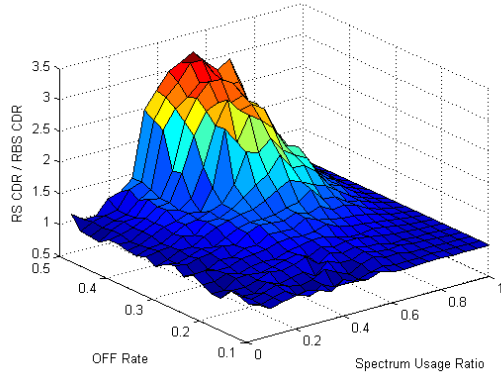
(b) RBS CDR with Various Traffic Parameters

Figure 3.13: CDR Comparison with Various PU Traffic Parameters

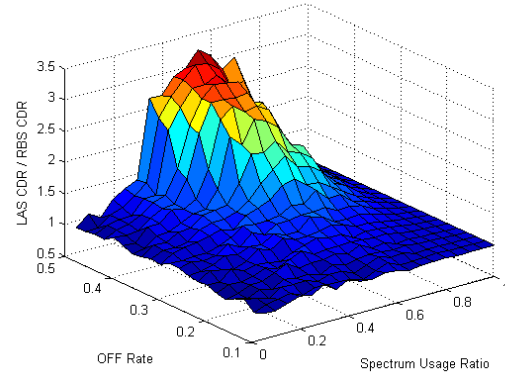
Figure 3.13(b) show CDR variations of RS and RBS with various PU traffic parameters. The RS and RBS CDR traces on Figure 3.12 represent slices of Figure 3.13(a) and Figure 3.13(b) with $\lambda_{OFF}=1/3$. In Figure 3.13(a) and Figure 3.13(b), RS CDR is lower than 20% and RBS CDR is lower than 15% in all ranges of OFF rate and PU usage ratio of 0.8 or less. While overall CDR of RS increases as λ_{OFF} increases, the CDR of RBS between 0.3 and 0.7 of PU spectrum ratio decreases as λ_{OFF} increases due to VSHs. Both RS and RBS CDR dramatically increase for PU spectrum usage ratio of 0.8 and higher. This increase happens because there are not enough spectrum holes for SUs due to the high spectrum usage of PUs.

To compare CDR performance among spectrum selection algorithms, we measure and calculate the CDR ratios of RS/RBS, LAS/RBS, and TPS/RBS. Because RBS has relatively stable and superior performance result with various traffic parameters, we choose RBS as a comparison base. In comparison results, the ratios greater than 1 mean that RBS

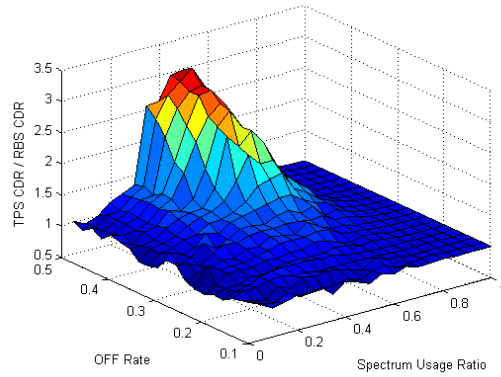
has superior performance. In case of RS and LAS comparisons in Figure 3.14(a) and Figure 3.14(b), the ratios are greater than 1 in all ranges. This means that RBS algorithm has longer undisrupted connection times with various traffic parameters when compared with RS and LAS. Between PU spectrum usage ratios 0 and 0.3, the CDR ratios increase slowly. Especially, RBS CDR has longer undisrupted connection times between PU spectrum usage ratios 0.3 and 0.9. Beyond PU spectrum usage ratio of 0.9, the CDR ratios converge on 1 because there are no spectrum holes for SUs. In comparison of TPS with RBS in Figure 3.14(c), TPS has better performance between PU spectrum usage ratios 0.3 and 0.7 with $\lambda_{OFF} \geq 0.25$ by initiating VSHs more aggressively than TBS. The comparison results rapidly converge to 1 between PU spectrum usage ratios 0.7 and 0.8.



(a) CDR Comparison with RS/RBS



(b) CDR Comparison with LAS/RBS



(c) CDR Comparison with TPS/RBS

Figure 3.14: CDR Comparison with RBS

CHAPTER 4

CONCLUSIONS AND FUTURE WORK

In this thesis, we propose two dynamic radio resource assignment schemes: *Adaptive Channel Hopping* in wireless sensor networks and *Voluntary Spectrum Handoff* in cognitive radio networks.

For interference robust sensor networks, a simple and reliable adaptive channel hopping scheme with standard compatibility is introduced. The proposed adaptive channel hopping method is designed to avoid the interference from other nodes and technologies on the ISM band based through link quality estimation. We propose algorithms for parent and child nodes to avoid interference using two messages with a three-way handshake and three timeout values to ensure channel locking. To minimize channel hopping latency, group members use an adaptive channel hopping sequence. In the comparison of each channel selection algorithm, ALQI has superior performance to RS and SS in all ranges and conditions. We have introduced a novel spectrum handoff scheme called voluntary spectrum handoff to minimize secondary user's disruption periods during spectrum handoff. To determine voluntary spectrum handoff time, we define spectrum lifetime which is estimated by two spectrum selection algorithms: Transition Probability Selection (TPS) and Reliability Based Selection (RBS). Thus, two spectrum selection algorithms are based on primary user spectrum usage estimation. For spectrum usage estimation, we propose to use a fixed

sensing window and a variable history window. The simulation results show that secondary users can reduce forced spectrum handoff counts with voluntary spectrum handoffs. With the reduced forced spectrum handoffs, secondary users can have longer undisrupted connection times. In the comparisons of each spectrum selection algorithm, while TPS has superior performance on DM, RBS has superior performance on IM and HM. On the performance comparison of various PU traffic parameters, RBS shows superior performance on various PU spectrum usage ratios.

With the radio resource management schemes (ACH and VSH), the sensor networks can minimize channel hopping latency and maintain robust communication in interfered environments, and secondary users in cognitive radio networks can have longer undisrupted connection times.

For the future work of Adaptive Channel Hopping, we would like to measure channel hopping latency and packet delivery ratio with hardware implementation in various interference environments. On the future of Voluntary Spectrum Handoff, we would like to explore an estimation of PU spectrum usage distributions from real world data sets, such as cellular and WiFi usage statistics, to build more realistic system models with voluntary spectrum handoffs on application traffic.

BIBLIOGRAPHY

- [1] Jens Zander, Radio Resource Management in Future Wireless Networks: Requirements and Limitations, IEEE Communications Magazine, August 1997.
- [2] Mohamed Hossam Ahmed, Alagan Anpalagan, Kwang-Cheng Chen, Zhu Han, and Ekram Hossain, Fairness in Radio Resource Management for Wireless Networks, EURASIP Journal on Wireless Communications and Networking, Article ID 642878, 3 pages, Volume 2009.
- [3] Institute of Electrical and Electronic Engineers, IEEE STD 802.15.4, 7 June 2006.
- [4] ZigBee Alliance, ZigBee Specifications, ZigBee Document 053474r17, January 17, 2008.
- [5] Ryan Winfield Woodings and Mark Gerrior, Avoiding Interference in the 2.4-GHz ISM Band, <http://www.wirelessnetdesignline.com/howto/60401206>.
- [6] ZigBee Alliance, ZigBee and Wireless Frequency Coexistances, ZigBee White Paper, June 2007.
- [7] Chulho Won, Jong-Hoon Youn, Hesham Ali, Hamid Sharif, and Jitender Deogun, Adaptive Radio Channel Allocation for Supporting Coexistence of 802.15.4 and 802.11b, IEEE Vehicular Technology Conference Vol.4 pp.2522-2526, Sep. 2005.
- [8] Razvan Musaloiu-E. and Andreas Terzis, Minimising the effect of WiFi interference in 802.15.4 wireless sensor networks, Int. J. Sensor Networks, Vol. 3, No. 1, 2008.
- [9] Aamir Mahmood, Frequency hopping in wireless sensor networks, MS Thesis, HELSINKI UNIVERSITY OF TECHNOLOGY, March 2009.
- [10] Soo Young Shin, Hong Seong Park, and Wook Hyun Kwon, Mutual interference analysis of IEEE 802.15.4 and IEEE 802.11b, Computer Networks Volume 51, Issue 12, 22 August 2007.
- [11] G. Simon, P. Volgyesi, M. Maroti, and A. Ledeczi, Simulation-based optimization of communication protocols for large-scale wireless sensor networks, IEEE Aerospace Conference, Vol3 pp.1339-1346, March 2003.

- [12] Kannan Srinivasan and Philip Levis, RSSI Is Under-Appreciated, In Proceedings of the Third Workshop on Embedded Networked Sensors (EmNets), 2006.
- [13] Texas Instruments, MSP430 Mixed Signal Microcontroller, July 2001.
- [14] Chipcon AS SmartRF CC2420 Preliminary Datasheet (rev 1.2), 2004-06-09.
- [15] E. Felemban, S. Vural, R. Murawski, E. Ekici, K. Lee, Y. Moon, and S. Park, "Samac: A cross-layer communication protocol for sensor networks with sectorized antennas," in Submitted to IEEE Trans. on Mobile Computing.
- [16] National Telecommunications and Information Administration, United States Frequency Allocations, <http://www.ntia.doc.gov/osmhome/allochrt.PDF>.
- [17] FCC Spectrum Policy Task Force, Report of the spectrum efficiency group, Nov., 2002.
- [18] Simon Haykin, Cognitive radio: brain-empowered wireless communications, IEEE Journal on Selected Areas in Communications, pp201- 220, Feb. 2005
- [19] Ian F. Akyildiz, Won-Yeol Lee, Mehmet C. Vuran, Shantidev Mohanty, NeXt generation/dynamic spectrum access/cognitive radio wireless networks: A survey, Computer Networks Journal (Elsevier), Vol. 50, No. 13, pp. 2127-2159, September 2006
- [20] Milind M. Buddhikot Understanding Dynamic Spectrum Access: Models, Taxonomy and Challenges, IEEE DySPAN 2007, April 2007
- [21] R. W. Thomas, L. A. DaSilva, and A. B. Mackenzie, Cognitive Networks, IEEE DySPAN 2005, Nov. 2005, pp. 352-60.
- [22] Ryan W. Thomas, Daniel H. Friend, Luiz A. DaSilva, and Allen B. MacKenzie, Cognitive Networks: Adaptation and Learning to Achieve End-to-End Performance Objectives, IEEE Communications Magazine, Volume 44, Issue 12, pp51-57, December 2006
- [23] Xiuhua FU, Wenan ZHOU, Junli XU, Junde SONG, Extended Mobility Management Challenges over Cellular Networks combined with Cognitive Radio by using Multi-hop Network, International Conference on SNPD 2007, pp. 683-688, July 2007
- [24] Hyoil Kim and Kang G. Shin, Efficient Discovery of Spectrum Opportunities with MAC-Layer Sensing in Cognitive Radio Networks, IEEE Transactions on Mobile Computing 2007
- [25] Guang-Hua Yang, Haitao Zheng, Jun Zhao, Li V.O.K., Adaptive Channel Selection Through Collaborative Sensing, IEEE International Conference on Communications, June 2006

- [26] L. Ma, X. Han, C.-C. Shen, Dynamic open spectrum sharing MAC protocol for wireless ad hoc network, *IEEE DySPAN 2005*, pp. 203-213, November 2005
- [27] Sudhir Srinivasa and Syed Ali Jafar, The Throughput Potential of Cognitive Radio: A Theoretical Perspective, *IEEE Communications Magazine*, May 2007
- [28] S. Krishnamurthy, M. Thoppian, S. Venkatesan, R. Prakash, Control channel based MAC-layer configuration, routing and situation awareness for cognitive radio networks, *IEEE MILCOM 2005*, October 2005.
- [29] Papadimitratos P., Sankaranarayanan S., Mishra A., A bandwidth sharing approach to improve licensed spectrum utilization, *IEEE Communications Magazine*, Volume 43, Issue 12, pp. 10-14, December 2005
- [30] Mark Girolami and Chao He, Probability Density Estimation from Optimally Condensed Data Samples, *IEEE Transactions on Pattern Analysis and Machine Intelligence*, VOL. 25, OCTOBER 2003
- [31] M.M. Buddhikot, P. Kolody, S. Miller, K. Ryan, J. Evans, DIMSUMNet: new directions in wireless networking using coordinated dynamic spectrum access, *IEEE WoWMoM 2005*, pp. 78-85, June 2005
- [32] Ileri, O. Samardzija, D. Mandayam, N.B., Demand responsive pricing and competitive spectrum allocation via a spectrum server, *IEEE International Symposium on DySPAN 2005*.
- [33] Marvin Rausand and Arnljot Hyland, *System Reliability Theory: Models, Statistical Methods, and Applications*, Wiley-Interscience, 2003
- [34] J. Zhao, H. Zheng, G.-H. Yang, Distributed coordination in dynamic spectrum allocation networks, *IEEE DySPAN 2005*, November 2005, pp. 259-268.